

Analytical results on quantum interference and magnetoconductance for strongly localized electrons in a magnetic field: exact summation of forward-scattering paths

Yeong-Lieh Lin

*Department of Physics, The University of Michigan, Ann Arbor, Michigan 48109-1120
and Department of Physics, West Virginia University, Morgantown, West Virginia 26506-6315**

Franco Nori

Department of Physics, The University of Michigan, Ann Arbor, Michigan 48109-1120
and Institute for Theoretical Physics, University of California, Santa Barbara, California 93106-4030
(November 6, 2018)*

We study quantum interference effects on the transition strength for strongly localized electrons hopping on two-dimensional (2D) square and three-dimensional (3D) cubic lattices in the presence of a magnetic field. These effects arise from the interference between phase factors associated with different electron paths connecting two distinct sites. For electrons confined on a square lattice, with and without disorder, we obtain *closed-form* expressions for the tunneling probability, which determines the conductivity, between two *arbitrary* sites by exactly summing the corresponding phase factors of *all* forward-scattering paths connecting them. By analytically summing paths which allow backward excursions in the forward-scattering direction, we find that the interference patterns between the dominant winding paths are not drastically different from those between the directed paths. An *analytic field-dependent* expression, valid in *any dimension*, for the magnetoconductance (MC) is derived. A *positive* MC is clearly observed when turning on the magnetic field. In 2D, when the strength of \mathbf{B} reaches a certain value, which is inversely proportional to twice the hopping length, the MC is increased by a factor of two compared to that at zero field. The periodicity in the flux of the MC is found to be equal to the superconducting flux quantum $hc/2e$. We also investigate transport on the much less-studied and experimentally important 3D cubic lattice case, where it is shown how the interference patterns and the small-field behavior of the MC vary according to the orientation of the applied field \mathbf{B} . At very small fields, for two sites diagonally separated a distance r , we find that the MC behaves as: rB in quasi-1D systems, $r^{3/2}B$ in 2D with $\mathbf{B} = (0, 0, B)$, and rB [$r^{3/2}B$] in 3D with \mathbf{B} parallel [perpendicular] to the $(1, 1, 1)$ direction. Furthermore, for a 3D sample, the effect on the low-flux MC due to the randomness of the angles between the hopping direction and the orientation of \mathbf{B} is examined analytically.

PACS numbers: 72.20.Dp, 72.10.Bg

I. INTRODUCTION

Electrons moving on a lattice immersed in a magnetic field have attracted much attention due to their relevance to many physical problems. In particular, quantum interference (QI) effects between different electron paths in disordered electron systems have been a subject of intense study because they play an important role in quantum transport. For instance, the QI of closed loops and their time-reversed paths is central to weak-localization phenomena.¹ Indeed, during the past decade and half, many fascinating phenomena—including universal conductance fluctuations as well as magnetic-field and spin-orbit scattering effects on the conductivity—observed in the *weakly* localized, metallic regime have been understood in terms of the QI between different Feynman diffusive paths in backscattering loops (i.e., paths bringing an electron back to the starting point). Recently, interest has grown in the effects of a magnetic field on *strongly* localized electrons^{2–9} with variable-range hopping (VRH) where striking QI phenomena has been observed in mesoscopic and macroscopic insulators or strongly disordered compounds: anomalous magnetoresistance, pronounced conductance fluctuations, Aharonov-Bohm oscillations with periods of hc/e and $hc/2e$, and the Hall effect. This strongly localized regime^{2–9} is less well-understood than the weak-localization case.

In the strongly localized regime, the major mechanism for transport is thermally activated hopping between the localized sites. In the VRH introduced by Mott,¹⁰ localized electrons, whose wavefunctions decay exponentially with a localization length ξ , hop a distance which is many times larger than ξ . As a result of the balance between the probabilities for hopping and thermal activation, Mott derived that in d dimensions the hopping length changes with temperature as $\xi(T_0/T)^{1/(d+1)}$, where T_0 is a characteristic temperature. Therefore, the lower the temperature is, the further away the electron tunnels in order to find a localized site of closer energy.

According to the “critical path analysis”¹¹ arguments, the conductance of the sample is governed by one critical hopping event. During this critical phonon-assisted tunneling process, the electron traverses many other impurities since the hopping length is very large at low temperatures. While encountering these intermediate scatterers, the electron preserves its phase memory. This elastic multiple-scattering is the origin of the QI effects associated with a single hopping event between the initial (i) and final (f) sites. The overall tunneling amplitude T_{if} between the sites i and f is therefore the sum of the contributions from all possible paths connecting them.^{2,3} In other words, the tunneling probability of one distant hop is determined by the interference of many electron paths between i and f . This leads to Mott’s law for the temperature dependence of the conductivity in d dimensions:¹⁰

$$\sigma(T) \sim |T_{if}|^2 \exp \left[- \left(\frac{T_0}{T} \right)^{\frac{1}{d+1}} \right].$$

It is worthwhile to note that, in the limit of strong localization, the dominant contribution to T_{if} comes from the shortest paths between i and f (i.e., the “directed path model”). In other words, only interference between *forward-scattering* paths need to be taken into account. This is in contrast with weak localization which results from *backscattering* processes on closed paths. The focus of this paper is on the QI effects on T_{if} and relevant physical quantities due to the presence of an external magnetic field. We will use the model proposed in Ref. 3, which is used in most of the recent theoretical work in this area. In this model, the impurities are arranged on a regular square (cubic) lattice in 2D (3D) and a nearest-neighbor tight-binding Anderson Hamiltonian is employed.

In this work we investigate the QI of strongly localized electrons by doing *exact* summations over *all* forward-scattering paths between two *arbitrary* sites. We derive compact *closed-form* expressions for various physical quantities (e.g., the transition strength which determines the conductivity) for electrons propagating on a square lattice subject to an external magnetic field, with and without random impurities. We also obtain an explicit formula for an experimentally important case that has been much less studied theoretically so far: the interference between paths on a 3D cubic lattice.

In the disordered case, by analytically computing the moments for the tunneling probability and employing the replica method, we derive *analytic* results for the magnetoconductance (MC) in terms of *sums-over-paths*, which are applicable in *any dimension*. Our explicit field-dependent expressions for the MC provide a precise description of the MC in terms of the magnetic flux. A *positive* MC, with a saturation value slightly larger than twice the MC at zero field, is observed when turning on the field \mathbf{B} . In 2D, the saturated value of the magnetic field B_{sa} (i.e., the first field that makes the MC become twice the value at zero field) is inversely proportional to twice the hopping length: the larger the system is, the smaller B_{sa} will be. In other words, as soon as the system, with hopping distance r , is penetrated by a total flux of $(r/8)(hc/e)$, the MC reaches the saturation value. The period of oscillation of the MC is found to be equal to $hc/2e$, which is the superconducting flux quantum.

Furthermore, at very small fields, for two sites diagonally separated a distance r , the MC scales as follows: (i) rB for quasi-1D ladder-type geometries with $\mathbf{B} = (0, 0, B)$, (ii) $r^{3/2}B$ in 2D with $\mathbf{B} = (0, 0, B)$, (iii) rB in 3D with \mathbf{B} parallel to the $(1, 1, 1)$ direction, and (iv) $r^{3/2}B$ in 3D with \mathbf{B} perpendicular to the $(1, 1, 1)$ direction.

The general expressions presented here: (i) *contain, as particular cases*, several QI results^{2–8} derived during the past decade (often by using either numerical or approximate methods), (ii) include QI to arbitrary points (m, n) on a square lattice, instead of only diagonal sites (m, m) , (iii) focus on 2D *and* 3D lattices, and (iv) can be extended to also include *backward* excursions (e.g., side windings) in the directed paths.

Exact results in this class of directed-paths problems are valuable and can be useful when studying other systems, for instance: (1) directed polymers in a disordered substrate (see, e.g., Refs. 12 and 13), (2) interfaces in 2D (see, for instance, Ref. 14), (3) light propagation in random media,^{15,16} and (4) charged bosons in 1D.¹⁷

To study the magnetic field effects on the tunneling probability of strongly localized electrons, we start from the tight-binding Hamiltonian

$$H = W \sum_i c_i^\dagger c_i + V \sum_{\langle ij \rangle} c_i^\dagger c_j \exp(iA_{ij}), \quad (1)$$

where $\langle ij \rangle$ refers to the nearest-neighbor sites and the phase $A_{ij} = 2\pi \int_i^j \mathbf{A} \cdot d\mathbf{l}$ is 2π times the line integral of the vector potential along the bond from i to j in units of the normal flux quantum hc/e . In the strongly localized regime, $V/W \ll 1$, the electron energy can be set to zero.^{4,6} Consider two states, localized at sites i and f which are r bonds apart. By using a locator expansion, the transition amplitude (Green’s function) T_{if} between these two states can be expressed as^{2–8}

$$T_{if} = \sum_{l=0}^{\infty} W \left(\frac{V}{W} \right)^{r+2l} S^{(r+2l)}, \quad (2)$$

where

$$S^{(r+2l)} = \sum_{\substack{\text{All } (r+2l)\text{-step paths } \Gamma \\ \text{connecting sites } i \text{ and } f}} e^{i\Phi_\Gamma}, \quad (3)$$

and Φ_Γ is the sum over phases of the bonds on the path Γ of $r+2l$ steps connecting sites i and f . In general, Γ contains closed loops. In the strongly localized regime (i.e., $V/W \ll 1$), the dominant contribution to T_{if} is $W(V/W)^r S^{(r)}$, where

$$S^{(r)} = \sum_{\substack{\text{All directed paths } \Gamma \\ \text{of } r \text{ steps on a lattice}}} e^{i\Phi_\Gamma}, \quad (4)$$

In other words, only the shortest-length paths (with *no* backward excursions) connecting them are taken into account, namely, the *directed-path model* of Refs. 2-8. This directed-path model provides an excellent approximation to T_{if} since $(V/W)^2$ is quite small in the extremely localized regime.²⁻⁸ It is important to stress that the *conductivity*²⁻⁵ between i and f is proportional to $|T_{if}|^2$.

Quantum interference, contained in $S^{(r+2l)}$, arises because the phase factors of different paths connecting the initial and final sites interfere with each other. We will first focus on the computation of $S^{(r)}$, which is the essential QI quantity for electrons deep in the localized regime. In 2D, we also analytically compute $S^{(r+2)}$ which becomes important when electrons are not so strongly localized.

This paper is organized as follows. In Sec. II, we study QI on a square lattice under a uniform potential, which is related to the decay of gap states into the bulk.² Here we derive an elegant, general, and very compact closed-form expression for $S^{(r)}$. Intriguing properties associated with the behavior of $S^{(r)}$ on diagonal sites are discussed in detail. It will be shown later (in section III) that the effect of a magnetic field on the MC is governed by the behavior of $S^{(r)}$. As a step towards the understanding of interference between non-directed paths, we also go beyond the directed-path model by exactly computing analytic results for $S^{(r+2)}$.

In Sec. III, we investigate the tunneling in a random impurity potential, which is relevant to the conductivity of, for example, lightly doped semiconductors and strongly disordered compounds.² Closed-form results for the tunneling probability, which determines the conductivity, are obtained. We then analytically compute the moments for the tunneling probability. From them, we derive analytic field-dependent expressions, valid in any dimension, for the MC. The full behavior of the MC as a function of the magnetic flux—including the scaling in the low-field limit and the occurrence of saturation—is discussed in detail. The close relationship between the QI quantity $S^{(r)}$ and the corresponding MC is illustrated. Comparison of our results with experimental observation and other theoretical work is also made.

In Sec. IV, we examine the QI on a 3D cubic lattice and provide a general formula for $S^{(r)}$. We show how the interference patterns and the small-field behavior of the MC vary according to the orientation of the applied field. Furthermore, we investigate the effect on the low-flux MC due to the randomness the angles between the directions of the critical hops and the orientation of the applied field.

In Sec. V, we conclude by addressing several relevant issues and summarize our results.

II. QUANTUM INTERFERENCE ON A TWO-DIMENSIONAL SQUARE LATTICE

A. Exact summation of forward-scattering paths: $S^{(r)}$

Let (m, n) denote the site coordinates. Without loss of generality, we choose $(0, 0)$ to be the initial site and focus on $m, n \geq 0$. For forward-scattering paths of r steps, which exclude backward excursions (i.e., only moving upward and to the right is allowed), ending sites (m, n) satisfy $m + n = r$. Let $S_{m,n}$ ($=S^{(r)}$) be the sum over all directed paths of r steps on which an electron can hop from the origin to the site (m, n) , each one weighted by its corresponding phase factor. Employing the symmetric gauge

$$\mathbf{A} = \frac{B}{2}(-y, x),$$

and denoting the flux through an elementary plaquette (i.e., with an area corresponding to the square of the average distance, which is typically equal to or larger than the localization length ξ , between two impurities) by $\phi/2\pi$, it is straightforward to construct the recursion relation:

$$S_{m,n} = e^{-in\phi/2} S_{m-1,n} + e^{im\phi/2} S_{m,n-1}. \quad (5)$$

This equation states that the site (m, n) can be reached by taking the r th step from neighboring sites to the left or below. The factors in front of the S 's, namely, $\exp(-in\phi/2)$ and $\exp(im\phi/2)$, account for the presence of the magnetic field. Enumerating the recursion relations for $S_{k_n,n}$ ($k_n = m-1, m-2, \dots, 0$) successively and using $S_{0,n} = 1$ for any n , we obtain the following relation

$$S_{m,n} = \sum_{k_n=0}^m e^{ik_n\phi/2} e^{-i(m-k_n)n\phi/2} S_{k_n,n-1}. \quad (6)$$

Here $S_{m,n}$ is expressed as a sum of the S 's one row below (i.e., on the line $y = n-1$). The physical meaning of Eq. (6) is clear: the site (m, n) can be reached by moving one step upward from sites $(k_n, n-1)$ with $0 \leq k_n \leq m$, acquiring the phase $ik_n\phi/2$; then traversing $m - k_n$ steps from (k_n, n) to (m, n) , each step with a phase $-in\phi/2$. By applying Eq. (6) recursively (and utilizing $S_{m,0} = 1$ for any m), $S_{m,n}$ for $m, n \geq 1$ can be written as

$$S_{m,n}(\phi) = e^{-imn\phi/2} L_{m,n}(\phi), \quad (7)$$

where

$$\begin{aligned} L_{m,n}(\phi) &= \sum_{k_n=0}^m \sum_{k_{n-1}=0}^{k_n} \cdots \sum_{k_1=0}^{k_2} e^{i(k_1 + \cdots + k_{n-1} + k_n)\phi} \\ &= \prod_{j=1}^n \sum_{k_j=0}^{k_{j+1}} e^{ik_j\phi}, \end{aligned} \quad (8)$$

with $k_{n+1} \equiv m$. If we use the Landau gauge instead, the expression for the sum-over-paths $S^{(r)}$ will read $L_{m,n}$; namely, $S_{m,n}$ employs the Symmetric gauge, while $L_{m,n}$ uses the Landau gauge. Notice that each term in the summand corresponds to the overall phase factor associated with a directed path. In the absence of the magnetic flux ($\phi = 0$),

$$\begin{aligned} S_{m,n}(0) &= \sum_{k_n=0}^m \sum_{k_{n-1}=0}^{k_n} \cdots \sum_{k_1=0}^{k_2} 1 \\ &= C_m^{m+n} = \frac{(m+n)!}{m!n!} \equiv N, \end{aligned} \quad (9)$$

which is just the total number of r -step paths between $(0, 0)$ and (m, n) .

After some calculations we obtain one of our main results, a very compact and elegant closed-form expression for $S_{m,n}(\phi)$:

$$S_{m,n}(\phi) = \frac{F_{m+n}(\phi)}{F_m(\phi) F_n(\phi)}, \quad (10)$$

where

$$F_m(\phi) = \prod_{k=1}^m \sin \frac{k}{2} \phi. \quad (11)$$

Notice that the symmetry $S_{m,n} = S_{n,m}$ [apparent in Eq. (10)] is due to the square lattice geometry. Moreover, we also obtain

$$L_{m,n}(\phi) = \frac{\prod_{k=1}^{m+n} (1 - e^{ik\phi})}{[\prod_{k=1}^m (1 - e^{ik\phi})][\prod_{k=1}^n (1 - e^{ik\phi})]}. \quad (12)$$

Previous work on QI in the VRH regime obtained particular cases, mostly numerical, of sums to diagonal points $S_{m,m}$, while the general result Eq. (10) is valid for arbitrary (e.g., non-diagonal) sites.

To illustrate the quantum interference originating from sums over phase factors associated with directed paths, we show the five possible ending sites (m, n) for $r = 4$ and their corresponding $S_{m,n}$ in Fig. 1(a). In addition, the six different paths connecting $(0, 0)$ and $(2, 2)$ and their separate phase factor contributions to $S_{2,2}$ are shown in Fig. 1(b).

B. Low-flux limit

In the very-low-flux limit $\phi \ll 1$, the logarithm of $S_{m,n}$, calculated exactly to order ϕ^2 , is

$$\ln S_{m,n}(\phi) = \ln N - \frac{1}{24} m n (m + n + 1) \phi^2. \quad (13)$$

Thus we obtain the familiar² harmonic shrinkage of the wave function with *explicit* expressions for all the prefactors. This result can be interpreted as follows. The effective ‘‘cigar-shape’’ area exposed to the field has an effective length l_{eff} :

$$l_{\text{eff}} \sim \sqrt{mn}$$

(i.e., the square root of the area enclosed by the paths) and an effective width w_{eff} :

$$w_{\text{eff}} \sim \sqrt{m+n}$$

(i.e., the square root of the length of the paths). For the special case $m = n = r/2$,

$$\ln S_{m,m}(\phi) = \ln \frac{r!}{[(r/2)!]^2} - \frac{1}{96} r^2 (r+1) \phi^2, \quad (14)$$

which is consistent with, and generalizes, the results in Ref. 4 since it gives the exact prefactor. Thus, the effective length is $\sim r$, while the effective width is $\sim \sqrt{r}$. Furthermore, for a ladder-type quasi-1D system, (e.g., $m = r - 1$ and $n = 1$), we have

$$\ln S_{r-1,1}(\phi) = \ln r - \frac{1}{24} (r^2 - 1) \phi^2. \quad (15)$$

In this case, the effective length and width are both $\sim \sqrt{r}$. This result remains valid for small values of n (narrow stripes or multiladders). The fourth-order contribution to $\ln S_{m,n}(\phi)$ can also be computed exactly as

$$\begin{aligned} \frac{mn}{103680} [& 10(6m^4 + 15m^3n + 20m^2n^2 + 15mn^3 + 6n^4) \\ & + 114(m^3 + 2m^2n + 2mn^2 + n^3) \\ & + 29(2m^2 + 3mn + 2n^2) + 9(m+n) + 5] \phi^4. \end{aligned}$$

C. Quantum interference on diagonal sites

Among the S 's for an even number of steps, those located along the diagonal corners contain the richest interference effects since the number of paths ending at (m, m) and the areas they enclose are both the largest. We therefore examine more closely the behavior of the quantities

$$I_{2m}(\phi) \equiv S_{m,m}(\phi) = \prod_{k=1}^m \frac{\sin \frac{m+k}{2} \phi}{\sin \frac{k}{2} \phi}. \quad (16)$$

For irrational flux ϕ , it can be proved that $-1 < I_{2m} < 1$ for any m . A *particular case* (asymptotic behavior) of our very compact general expression Eq. (16) for I_{2m} is investigated in detail by Fishman, Shapir, and Wang in Ref. 6. For $\phi = 2\pi s/t$ (s and t are positive integers with $1 \leq s < t$ and s being prime to t), we obtain ($n \geq 0$) for $m < t$

$$I_{2(m+nt)} = \frac{(-1)^{stn} (2n)!}{n! n!} I_{2m}, \quad (17)$$

and

$$I_{2nt} = (-1)^{stn} \frac{(2n)!}{(n!)^2}. \quad (18)$$

Furthermore, for those m satisfying

$$\frac{t}{2} \leq m \leq t - 1, \quad (19)$$

$$I_{2(m+nt)} = 0. \quad (20)$$

In other words, the zeros of $I_{2m}(\phi)$ are given by $\phi = 2\pi s/t$ for

$$\frac{m+1}{n+1} \leq t \leq \frac{2m}{2n+1}, \quad (21)$$

with

$$0 \leq n \leq \frac{m-1}{2}, \quad (22)$$

and the s 's are prime to each allowed t . From a physical viewpoint, these flux values produce the complete cancelation of all phase factors (i.e., *fully destructive interference*) and result in the *vanishing* of the tunneling probability (and conductivity). Indeed, we will see in section III that if we also consider the effects of the on-site impurity scattering, these flux values lead to the largest (i.e., saturated) value for the positive MC.

In Fig. 2, we show the zeros for $I_2, I_4, I_6, \dots, I_{40}$ obtained by using Eqs. (21) and (22). Note that the smallest value of $\phi/2\pi$ satisfying $I_{2m}(\phi) = 0$ is always $1/2m$ and the number of zeros rapidly increases when m becomes larger.

The I_{2m} can be expressed as sums of trigonometric cosines. For instance, the first few ones are (with $\theta \equiv \phi/2$):

$$I_2 = 2 \cos \theta,$$

$$I_4 = 2 + 2 \cos 2\theta + 2 \cos 4\theta,$$

$$I_6 = 6 \cos \theta + 6 \cos 3\theta + 4 \cos 5\theta + 2 \cos 7\theta + 2 \cos 9\theta,$$

$$I_8 = 8 + 14 \cos 2\theta + 14 \cos 4\theta + 10 \cos 6\theta + 10 \cos 8\theta + 6 \cos 10\theta + 4 \cos 12\theta + 2 \cos 14\theta + 2 \cos 16\theta,$$

$$I_{10} = 40 \cos \theta + 38 \cos 3\theta + 36 \cos 5\theta + 32 \cos 7\theta + 28 \cos 9\theta + 22 \cos 11\theta + 18 \cos 13\theta \\ + 14 \cos 15\theta + 10 \cos 17\theta + 6 \cos 19\theta + 4 \cos 21\theta + 2 \cos 23\theta + 2 \cos 25\theta,$$

$$I_{12} = 58 + 110 \cos 2\theta + 110 \cos 4\theta + 102 \cos 6\theta + 96 \cos 8\theta + 84 \cos 10\theta + 78 \cos 12\theta + 64 \cos 14\theta \\ + 56 \cos 16\theta + 44 \cos 18\theta + 36 \cos 20\theta + 26 \cos 22\theta + 22 \cos 24\theta + 14 \cos 26\theta \\ + 10 \cos 28\theta + 6 \cos 30\theta + 4 \cos 32\theta + 2 \cos 34\theta + 2 \cos 36\theta,$$

$$I_{14} = 338 \cos \theta + 332 \cos 3\theta + 324 \cos 5\theta + 310 \cos 7\theta + 292 \cos 9\theta + 272 \cos 11\theta + 250 \cos 13\theta + 224 \cos 15\theta \\ + 200 \cos 17\theta + 174 \cos 19\theta + 150 \cos 21\theta + 126 \cos 23\theta + 106 \cos 25\theta + 84 \cos 27\theta + 68 \cos 29\theta + 52 \cos 31\theta \\ + 40 \cos 33\theta + 30 \cos 35\theta + 22 \cos 37\theta + 14 \cos 39\theta + 10 \cos 41\theta + 6 \cos 43\theta + 4 \cos 45\theta + 2 \cos 47\theta + 2 \cos 49\theta.$$

Notice that I_{2m} depends only on the even (odd) harmonics of θ when m is even (odd). $I_{2m}(\phi)$ obeys the following properties: (i) 2π (4π) periodicity in ϕ for even (odd) m , namely,

$$I_{4n}(\phi + 2\pi) = I_{4n}(\phi), \\ I_{4n+2}(\phi + 4\pi) = I_{4n+2}(\phi).$$

In other words, the period of I_{2m} corresponds to hc/e when m is even, and $2hc/e$ when m is odd. (ii) With m even

$$I_{2m}(2\pi - \phi) = I_{2m}(\phi)$$

for $0 \leq \phi \leq \pi$. Also

$$I_{2m}(\pi) = \frac{m!}{[(m/2)!]^2}.$$

(iii) With m odd

$$I_{2m}(2\pi \pm \phi) = -I_{2m}(\phi)$$

for $0 \leq \phi \leq 2\pi$.

From the properties described above, we can draw a general picture of the behavior of I_{2m} . Let $\Phi \equiv \phi/2\pi$. $I_{2m}(\Phi = 0) = (2m)!/(m!)^2$, which is a enormous number for large m . As the magnetic field is turned on, I_{2m} rapidly drops to its first zero at $\Phi = 1/2m$. I_{2m} then shows distinct behaviors depending on m .

For even m , I_{2m} exhibits many small-magnitude fluctuations around zero for $\frac{1}{2m} < \Phi < \frac{m-1}{2m}$. I_{2m} then monotonically climbs from 0 to a large positive value, $I_{2m}(\pi) = m!/[(m/2)!]^2$, for $\frac{m-1}{2m} \leq \Phi \leq \frac{1}{2}$. It is evident that $I_{2m}(\pi)$ is still very small compared to $I_{2m}(0)$. Within the period $0 \leq \Phi \leq 1$ (i.e., $0 \leq \phi \leq 2\pi$), I_{2m} has mirror symmetry with respect to $\Phi = 1/2$ (i.e., $\phi = \pi$).

For odd m , I_{2m} exhibits many small-magnitude fluctuations around zero for $\frac{1}{2m} < \Phi < \frac{2m-1}{2m}$. In addition, I_{2m} always equals 0 at $\Phi = 1/2$ (i.e., $\phi = \pi$). I_{2m} then monotonically drops from 0 to $-(2m)!/(m!)^2$ for $\frac{2m-1}{2m} \leq \Phi \leq 1$. For $0 \leq \Phi \leq 1$, I_{2m} has inversion symmetry with respect to $\Phi = 1/2$. Within the period $0 \leq \Phi \leq 2$ (i.e., $0 \leq \phi \leq 4\pi$), I_{2m} has mirror symmetry around $\Phi = 1$ (i.e., $\phi = 2\pi$). Recall that for any m , $-1 < I_{2m} < 1$, for irrational values of Φ .

In Fig. 3, we plot I_2 through I_{12} , I_{18} , I_{20} , I_{38} and I_{40} . These figures show very interesting interference patterns of I_{2m} and clearly reflect the general description given above. It is worthwhile to keep in mind that the properties embedded in $S_{m,n}$ described above play a central role in determining the behavior of the MC obtained in section III.

D. Exact summation of the dominant winding paths: $S^{(r+2)}$

Up to now, we have focused on the computation of $S^{(r)}$ and presented a detailed investigation of their properties. When the electrons are less strongly localized, the next higher-order contribution to T_{if} (i.e., $W(V/W)^{r+2}S^{(r+2)}$, which is the dominant term *including backward excursions*) becomes important. Therefore, quantum interference effects between phase factors of paths with backward recursions (i.e., moving downward and to the left is also included) need to be taken into consideration. Notice that paths in $S^{(r+2)}$, though include backscattering processes, do not involve closed loops enclosing flux (e.g., elementary square plaquettes).

In this section we present the computation of the second-order contribution, namely $S^{(r+2)}$, to the transition amplitude T_{if} . Let $P_{m,n}$ ($= S^{(r+2)}$) denote the sums over paths of $m+n+2$ steps starting from $(0,0)$ and ending at (m,n) . We assume that the electrons are confined on a square lattice with non-negative x and y coordinates. We can divide the contribution to $P_{m,n}$ into five parts.

First, hopping directly to site $(p,0)$, with $1 \leq p \leq m$, electrons take one step back to $(p-1,0)$, then hop $m-p+1+n$ steps to (m,n) . Second, hopping directly to site $(0,q)$, with $1 \leq q \leq n$, electrons take one step back to $(0,q-1)$, then hop $m+n-q+1$ steps to (m,n) . Third, directly hopping to site $(p,n+1)$, with $0 \leq p \leq m$, electrons move one-step downward to (p,n) gaining a phase factor $\exp(-ip\phi/2)$, then hop $m-p$ steps to (m,n) . Fourth, directly hopping to site $(m+1,q)$, with $0 \leq q \leq n$, electrons move one-step downward to (m,q) gaining a phase factor $\exp(iq\phi/2)$, then hop $n-q$ steps to (m,n) . Fifth, directly hopping to (p,q) with $1 \leq p \leq m$ and $1 \leq q \leq n$, electrons take one step back to either $(p-1,q)$ or $(p,q-1)$, accompanied by the phase factor $\exp(iq\phi/2)$ or $\exp(-ip\phi/2)$, then hop $m+n-p-q+1$ steps to the ending site (m,n) . Therefore $P_{m,n}$ can be written as

$$P_{m,n} = \sum_{p=1}^m B_{p-1,0 \rightarrow m,n} + \sum_{q=1}^n B_{0,q-1 \rightarrow m,n} + \sum_{p=0}^m S_{p,n+1} e^{-ip\phi/2} B_{p,n \rightarrow m,n} + \sum_{q=0}^n S_{m+1,q} e^{iq\phi/2} B_{m,q \rightarrow m,n} + \sum_{p=1}^m \sum_{q=1}^n S_{p,q} \left(e^{iq\phi/2} B_{p-1,q \rightarrow m,n} + e^{-ip\phi/2} B_{p,q-1 \rightarrow m,n} \right). \quad (23)$$

where $B_{p,q \rightarrow m,n}$ is the sum over phase factors of all directed paths (i.e., containing $m+n-p-q$ steps) starting from (p,q) and ending at (m,n) . After some calculation we obtain

$$B_{p,q \rightarrow m,n} = \exp \left\{ i \frac{[-(m-p)q + (n-q)p]\phi}{2} \right\} S_{m-p,n-q}. \quad (24)$$

By substituting Eq. (24) into Eq. (23), we derive

$$P_{m,n} = \sum_{p=1}^m e^{\frac{in(p-1)\phi}{2}} S_{m-p+1,n} + \sum_{q=1}^n e^{-\frac{im(q-1)\phi}{2}} S_{m,n-q+1} + e^{-\frac{imn\phi}{2}} \sum_{p=0}^m e^{\frac{i(n-1)p\phi}{2}} S_{p,n+1} + e^{\frac{imn\phi}{2}} \sum_{q=0}^n e^{-\frac{i(m-1)q\phi}{2}} S_{m+1,q} + \sum_{p=1}^m \sum_{q=1}^n S_{p,q} \left\{ e^{-i[(m-1)q-n(p-1)]\phi/2} S_{m-p+1,n-q} + e^{-i[m(q-1)-(n-1)p]\phi/2} S_{m-p,n-q+1} \right\}. \quad (25)$$

In the special case $m = n$,

$$\begin{aligned}
P_{m,m} = & 2 \sum_{j=1}^m \cos \left[\frac{m(m-j)\phi}{2} \right] S_{j,m} + 2 \sum_{j=0}^m \cos \left[\frac{(m^2 - mj + j)\phi}{2} \right] S_{j,m+1} + 2 \sum_{j=0}^{m-1} \cos \left(\frac{j\phi}{2} \right) S_{m-j,m-j} S_{j,j+1} \\
& + 2 \sum_{j=1}^{m-1} \sum_{k=0}^{j-1} S_{m-j,m-k} \left\{ \cos \left[\frac{(mj - mk - j)\phi}{2} \right] S_{j,k+1} + \cos \left[\frac{(mj - mk + k)\phi}{2} \right] S_{k,j+1} \right\}. \tag{26}
\end{aligned}$$

The explicit expressions for the first few $P_{m,m}$ are (with $\theta = \phi/2$):

$$\begin{aligned}
P_{1,1} &= 14 \cos \theta + 2 \cos 3\theta, \\
P_{2,2} &= 26 + 32 \cos 2\theta + 26 \cos 4\theta + 4 \cos 6\theta + 2 \cos 8\theta, \\
P_{3,3} &= 130 \cos \theta + 124 \cos 3\theta + 88 \cos 5\theta + 52 \cos 7\theta + 40 \cos 9\theta + 8 \cos 11\theta + 4 \cos 13\theta + 2 \cos 15\theta, \\
P_{4,4} &= 224 + 410 \cos 2\theta + 396 \cos 4\theta + 308 \cos 6\theta + 282 \cos 8\theta + 188 \cos 10\theta + 130 \cos 12\theta \\
&\quad + 76 \cos 14\theta + 58 \cos 16\theta + 14 \cos 18\theta + 8 \cos 20\theta + 4 \cos 22\theta + 2 \cos 24\theta, \\
P_{5,5} &= 1446 \cos \theta + 1386 \cos 3\theta + 1308 \cos 5\theta + 1176 \cos 7\theta + 1032 \cos 9\theta + 842 \cos 11\theta + 690 \cos 13\theta \\
&\quad + 542 \cos 15\theta + 398 \cos 17\theta + 264 \cos 19\theta + 180 \cos 21\theta + 108 \cos 23\theta + 80 \cos 25\theta \\
&\quad + 24 \cos 27\theta + 14 \cos 29\theta + 8 \cos 31\theta + 4 \cos 33\theta + 2 \cos 35\theta, \\
P_{6,6} &= 2518 + 4868 \cos 2\theta + 4808 \cos 4\theta + 4514 \cos 6\theta + 4238 \cos 8\theta + 3788 \cos 10\theta + 3466 \cos 12\theta \\
&\quad + 2938 \cos 14\theta + 2554 \cos 16\theta + 2074 \cos 18\theta + 1702 \cos 20\theta + 1298 \cos 22\theta + 1056 \cos 24\theta \\
&\quad + 736 \cos 26\theta + 536 \cos 28\theta + 356 \cos 30\theta + 244 \cos 32\theta + 148 \cos 34\theta + 110 \cos 36\theta \\
&\quad + 38 \cos 38\theta + 24 \cos 40\theta + 14 \cos 42\theta + 8 \cos 44\theta + 4 \cos 46\theta + 2 \cos 48\theta.
\end{aligned}$$

These $P_{m,m}$'s are plotted in Fig. 4. Note that $P_{m,m}$ depends only on the even (odd) harmonics of θ and has a period 2π (4π) for even (odd) m . The expressions for $P_{m,m}$ are obviously more complicated than the corresponding I_{2m} . However, by comparing Figs. 3 and 4, we find that the general features in the interference behaviors are surprisingly similar. We thus infer that the relevant physical quantities are not significantly changed by the addition of interference between the dominant winding paths.

III. EFFECTS OF DISORDER

A. Average of the tunneling probability

To incorporate the effects of random impurities, we now replace the on-site energy part in Eq. (1) (first term in H) by $\sum_i \epsilon_i c_i^\dagger c_i$, where the ϵ_i 's are now independent random variables. The Hamiltonian now takes the form

$$H = \sum_i \epsilon_i c_i^\dagger c_i + V \sum_{\langle ij \rangle} c_i^\dagger c_j \exp(iA_{ij}).$$

We have studied two commonly used models: (i) ϵ_i can take two values: $+W$ and $-W$ with equal probability; and (ii) ϵ_i is randomly chosen from a uniform distribution of width W and zero mean. We found that both models yield the same results for the MC.

We now start with the general case of the first model, namely, ϵ_i can have two values: $+W$ with probability μ and $-W$ with probability ν , where $\mu + \nu = 1$. Due to disorder, the transition amplitude becomes

$$T_{if} = W \left(\frac{V}{W} \right)^r J_{m,n},$$

with

$$J_{m,n} = \sum_{\Gamma} \left[\prod_{j \in \Gamma} \left(-\frac{W}{\epsilon_j} \right) \right] e^{i\Phi_{\Gamma}}, \tag{27}$$

where Γ runs over all directed paths of r steps connecting sites $(0,0)$ and (m,n) , and j over sites on each path. For all directed paths ending at (m,n) , electrons traverse $r = m + n$ sites (the initial site $(0,0)$ is excluded). Each site

visited now contributes an additional multiplicative factor of either +1 or -1 to the phase factor. Therefore, for a given path Γ , the probability for obtaining $\pm e^{i\Phi_\Gamma}$ is

$$P_\pm = \frac{(\mu + \nu)^r \pm (\mu - \nu)^r}{2}.$$

It is then clear that

$$\langle J_{m,n}(\phi) \rangle = (P_+ - P_-) S_{m,n}(\phi) = (\mu - \nu)^r S_{m,n}(\phi), \quad (28)$$

where $\langle \dots \rangle$ denotes averaging over all impurities.

By exploiting Eqs. (7) and (8), we derive the following general expressions valid for *any* μ and ν ,

$$\langle J_{m,n}^2(\phi) \rangle = (1 - \mathcal{P}) S_{m,n}(2\phi) + \mathcal{P} S_{m,n}^2(\phi), \quad (29)$$

where

$$\begin{aligned} \mathcal{P} &= P_+^N + P_-^N + \sum_{k=1}^{N-1} P_+^{N-k} P_-^k (C_k^N - 4C_{k-1}^{N-2}) \\ &= 1 - 4P_+ P_- = (\mu - \nu)^{2r}. \end{aligned} \quad (30)$$

Also, the disorder average of the tunneling probability (i.e., the transmission rate) $|J|^2 = JJ^*$ is

$$\langle |J_{m,n}(\phi)|^2 \rangle = (1 - \mathcal{P}) N + \mathcal{P} S_{m,n}^2(\phi). \quad (31)$$

The physical origin of Eqs. (29) and (31) becomes clearer by rewriting them as

$$\langle J_{m,n}^2(\phi) \rangle = S_{m,n}(2\phi) + \mathcal{P} S_{m,n}(\phi) [S_{m,n}(\phi) - C_{m,n}(\phi)] \quad (32)$$

and

$$\langle |J_{m,n}(\phi)|^2 \rangle = N + \mathcal{P} [S_{m,n}^2(\phi) - N], \quad (33)$$

where

$$C_{m,n}(\phi) = \frac{\prod_{k=1}^{m+n} \cos \frac{k}{2} \phi}{\left(\prod_{k=1}^m \cos \frac{k}{2} \phi \right) \left(\prod_{k=1}^n \cos \frac{k}{2} \phi \right)},$$

and we have used

$$S_{m,n}(2\phi) = S_{m,n}(\phi) C_{m,n}(\phi).$$

The first terms in Eqs. (32) and (33) account for contributions from pairs of identical paths:

$$\sum_{\Gamma} (\pm e^{i\Phi_\Gamma}) (\pm e^{i\Phi_\Gamma}) = \sum_{\Gamma} e^{2i\Phi_\Gamma} = S_{m,n}(2\phi)$$

in $\langle J_{m,n}^2 \rangle$, and

$$\sum_{\Gamma} (\pm e^{i\Phi_\Gamma}) (\pm e^{-i\Phi_\Gamma}) = \sum_{\Gamma} 1 = N$$

in $\langle |J_{m,n}|^2 \rangle$. The second terms in Eqs. (32) and (33) account for contributions from pairs of distinct paths. Note that $S_{m,n}(0) = N$ and $C_{m,n}(0) = 1$, when $\phi = 0$. We then have in the absence of magnetic flux

$$\langle J_{m,n}^2(0) \rangle = \langle |J_{m,n}(0)|^2 \rangle = N + \mathcal{P} N (N - 1). \quad (34)$$

Furthermore, in the special case $\mu = \nu = 1/2$, since $\mathcal{P} = 0$ we then obtain

$$\begin{aligned} \langle J_{m,n}(\phi) \rangle &= 0, \\ \langle J_{m,n}^2(\phi) \rangle &= S_{m,n}(2\phi), \\ \langle |J_{m,n}(\phi)|^2 \rangle &= N. \end{aligned}$$

B. Higher-order moments and general expressions for the first few leading terms

For $\mu = \nu = 1/2$ (the most studied case so far), we can obtain analytical expressions for the moments $\langle J_{m,n}^{2p}(\phi) \rangle$ and $\langle |J_{m,n}(\phi)|^{2p} \rangle$ for any value of p . Only a few of these will be presented here. From now on, $J(\phi)$ stands for $J_{m,n}(\phi)$ and $S(\phi)$ stands for $S_{m,n}(\phi)$. The derivation of these moments is given in appendix A.

$$\langle J^4(\phi) \rangle = 3S^2(2\phi) - 2S(4\phi), \quad (35.1)$$

$$\langle J^6(\phi) \rangle = 15S^3(2\phi) - 30S(2\phi)S(4\phi) + 16S(6\phi), \quad (35.2)$$

$$\langle J^8(\phi) \rangle = 105S^4(2\phi) - 420S^2(2\phi)S(4\phi) + 448S(2\phi)S(6\phi) + 140S^2(4\phi) - 272S(8\phi), \quad (35.3)$$

$$\begin{aligned} \langle J^{10}(\phi) \rangle &= 945S^5(2\phi) - 6300S^3(2\phi)S(4\phi) + 10080S^2(2\phi)S(6\phi) + 6300S(2\phi)S^2(4\phi) \\ &\quad - 12240S(2\phi)S(8\phi) - 6720S(4\phi)S(6\phi) + 7936S(10\phi), \end{aligned} \quad (35.4)$$

$$\begin{aligned} \langle J^{12}(\phi) \rangle &= 10395S^6(2\phi) - 103950S^4(2\phi)S(4\phi) + 221760S^3(2\phi)S(6\phi) + 207900S^2(2\phi)S^2(4\phi) \\ &\quad - 403920S^2(2\phi)S(8\phi) - 443520S(2\phi)S(4\phi)S(6\phi) - 46200S^3(4\phi) \\ &\quad + 523776S(2\phi)S(10\phi) + 269280S(4\phi)S(8\phi) + 118272S^2(6\phi) - 353792S(12\phi), \end{aligned} \quad (35.5)$$

$$\begin{aligned} \langle J^{14}(\phi) \rangle &= 135135S^7(2\phi) - 1891890S^5(2\phi)S(4\phi) + 5045040S^4(2\phi)S(6\phi) + 6306300S^3(2\phi)S^2(4\phi) \\ &\quad - 12252240S^3(2\phi)S(8\phi) - 20180160S^2(2\phi)S(4\phi)S(6\phi) - 4204200S(2\phi)S^3(4\phi) \\ &\quad + 23831808S^2(2\phi)S(10\phi) + 24504480S(2\phi)S(4\phi)S(8\phi) + 10762752S(2\phi)S^2(6\phi) \\ &\quad + 6726720S^2(4\phi)S(6\phi) - 32195072S(2\phi)S(12\phi) - 15887872S(4\phi)S(10\phi) \\ &\quad - 13069056S(6\phi)S(8\phi) + 22368256S(14\phi), \end{aligned} \quad (35.6)$$

and

$$\langle |J(\phi)|^4 \rangle = 2N(N-1) + S^2(2\phi), \quad (36.1)$$

$$\langle |J(\phi)|^6 \rangle = 2N(3N^2 - 9N + 8) + 3(3N - 4)S^2(2\phi), \quad (36.2)$$

$$\begin{aligned} \langle |J(\phi)|^8 \rangle &= 8N(3N^3 - 18N^2 + 41N - 34) + 8(9N^2 - 33N + 32)S^2(2\phi) \\ &\quad + 9S^4(2\phi) - 12S^2(2\phi)S(4\phi) + 4S^2(4\phi), \end{aligned} \quad (36.3)$$

$$\begin{aligned} \langle |J(\phi)|^{10} \rangle &= 8N(15N^4 - 150N^3 + 625N^2 - 1250N + 992) + 40(15N^3 - 105N^2 + 260N - 216)S^2(2\phi) \\ &\quad + 75(3N - 8)S^4(2\phi) - 20(15N - 44)S^2(2\phi)S(4\phi) + 20(5N - 16)S^2(4\phi), \end{aligned} \quad (36.4)$$

$$\begin{aligned} \langle |J(\phi)|^{12} \rangle &= 16N(45N^5 - 675N^4 + 4425N^3 - 15525N^2 + 28706N - 2212) \\ &\quad + 120(45N^4 - 510N^3 + 2295N^2 - 4702N + 3552)S^2(2\phi) + 30(135N^2 - 854N + 1440)S^4(2\phi) \\ &\quad + 225S^6(2\phi) - 120(45N^2 - 309N + 556)S^2(2\phi)S(4\phi) - 900S^4(2\phi)S(4\phi) \\ &\quad + 24(75N^2 - 555N + 1064)S^2(4\phi) + 900S^2(2\phi)S^2(4\phi) + 480S^3(2\phi)S(6\phi) \\ &\quad - 960S(2\phi)S(4\phi)S(6\phi) + 256S^2(6\phi), \end{aligned} \quad (36.5)$$

$$\begin{aligned} \langle |J(\phi)|^{14} \rangle &= 16N(315N^6 - 6615N^5 + 62475N^4 - 334425N^3 + 1057322N^2 - 1854160N + 1398016) \\ &\quad + 56(945N^5 - 1575N^4 + 110775N^3 - 401730N^2 + 732536N - 518464)S^2(2\phi) \\ &\quad + 1470(45N^3 - 495N^2 + 1920N - 2576)S^4(2\phi) + 11025(N - 4)S^6(2\phi) \\ &\quad - 840(105N^3 - 1239N^2 + 5096N - 7192)S^2(2\phi)S(4\phi) - 2940(15N - 64)S^4(2\phi)S(4\phi) \\ &\quad + 2940(15N - 68)S^2(2\phi)S^2(4\phi) + 3360(7N - 31)S^3(2\phi)S(6\phi) \\ &\quad + 56(525N^3 - 6615N^2 + 28784N - 42688)S^2(4\phi) - 448(105N - 493)S(2\phi)S(4\phi)S(6\phi) \\ &\quad + 1792(7N - 34)S^2(6\phi). \end{aligned} \quad (36.6)$$

These moments satisfy the consistency check $\langle J^{2p}(0) \rangle = \langle |J(0)|^{2p} \rangle$ and odd moments vanish by symmetry.

The moments provide an analytical view of the structure of the QI in the tunneling process. Since $|J|^2 = JJ^*$, each $|J|^2$ represents N *forward* paths to (m, n) , each one with its corresponding *reversed* path back to the origin. Also, $\langle |J(\phi)|^{2p} \rangle$, averages over the contributions of N^p such pairs of paths. In general, $\langle |J(\phi)|^{2p} \rangle$ consist of terms involving N^k ($k = 1, \dots, p$). The above explicit expressions for the moments will allow us to deduce general formulae for the first few leading (i.e., dominant) terms in the moments.

We first focus on the leading terms ($\propto N^p$), since they provide the most significant contribution to the moments when N is large. Recall that $S(0) = N$, therefore we need to consider all terms involving $S^{2k}(2\phi)N^{p-2k}$ in $\langle |J(\phi)|^{2p} \rangle$. We derive (see appendix B for more details)

$$\langle |J(0)|^{2p} \rangle = (2p-1)!! N^p, \quad (37)$$

$$\langle |J(\phi)|^{2p} \rangle = p! N^p \left\{ \sum_{k=0}^{\infty} \frac{(2k)! C_{2k}^p}{(2^k k!)^2} \left[\frac{S(2\phi)}{N} \right]^{2k} \right\}. \quad (38)$$

Furthermore, by considering all the second leading terms ($\propto N^{p-1}$), we obtain

$$\langle |J(0)|^{2p} \rangle = -\frac{1}{3} p(p-1) [(2p-1)!!] N^{p-1}, \quad (39)$$

$$\langle |J(\phi)|^{2p} \rangle = -\frac{p! N^{p-1}}{6} \left\{ \sum_{k=0}^{\infty} \frac{(2k+1)!}{(2^k k!)^2} \left[(3p+2k-3) C_{2k+1}^p + 2k C_{2k+2}^p \frac{S(4\phi)}{N} \right] \left[\frac{S(2\phi)}{N} \right]^{2k} \right\}. \quad (40)$$

Also, when $S(2p\phi) = 0$ with $p \geq 1$ (e.g., at $\phi = \pi/m$, $S_{m,m}(2p\phi) = 0$), the third leading terms ($\propto N^{p-2}$) in the moments are

$$\langle |J(0)|^{2p} \rangle = \frac{1}{90} p(p-1)(p-2)(5p+1) [(2p-1)!!] N^{p-2}, \quad (41)$$

$$\langle |J(\phi)|^{2p} \rangle = \frac{1}{72} p(p-1)(p-2)(9p+5)(p!) N^{p-2}. \quad (42)$$

The above general expressions for the moments are of value since they enable us to *analytically* obtain the dominant contributions to the quantity we are interested in: the magnetoconductance.

C. Analytical results for the magnetoconductance

We now use the replica method:

$$\langle \ln |J(\phi)|^2 \rangle = \lim_{p \rightarrow 0} \frac{\langle |J(\phi)|^{2p} \rangle - 1}{p} \quad (43)$$

to compute the log-averaged MC with respect to the zero-field log-averaged MC (denoted by L_{MC}), defined as

$$\begin{aligned} L_{MC} &\equiv \langle \ln |J(\phi)|^2 \rangle - \langle \ln |J(0)|^2 \rangle \\ &= \lim_{p \rightarrow 0} \frac{\langle |J(\phi)|^{2p} \rangle - \langle |J(0)|^{2p} \rangle}{p}. \end{aligned} \quad (44)$$

Taking into account only the first leading terms in the moments, shown in Eqs. (37) and (38), we derive the L_{MC} as

$$L_{MC} = \ln 2 - \sum_{k=1}^{\infty} \frac{(2k-1)!}{(2^k k!)^2} \left[\frac{S(2\phi)}{N} \right]^{2k}, \quad (45)$$

where we have

$$\sum_{k=1}^{\infty} \frac{(2k-1)!}{(2^k k!)^2} = \ln 2. \quad (46)$$

Exploiting the following identity¹⁸ for $0 < x \leq 1$

$$\cosh^{-1} \frac{1}{x} = \ln \frac{2}{x} - \sum_{k=1}^{\infty} \frac{(2k-1)!}{(2^k k!)^2} x^{2k},$$

which reduces to Eq. (46) for $x = 1$, we thus obtain a very concise exact expression for the L_{MC} as

$$L_{MC} = \begin{cases} \cosh^{-1} \frac{N}{|S(2\phi)|} - \ln \frac{N}{|S(2\phi)|} & \text{when } S(2\phi) \neq 0 \\ \ln 2 & \text{when } S(2\phi) = 0 \end{cases} \quad (47)$$

$$= \ln \left[1 + \sqrt{1 - \left(\frac{S(2\phi)}{N} \right)^2} \right]. \quad (48)$$

The typical MC of a sample

$$G(\phi) = \exp(\langle \ln |J(\phi)|^2 \rangle)$$

is then given by, normalized by the zero-field MC $G(0)$,

$$\frac{G(\phi)}{G(0)} = \exp(L_{MC}) = 1 + \sqrt{1 - \left[\frac{S(2\phi)}{N} \right]^2}. \quad (49)$$

Eq. (49) is one of our main results. It provides a concise closed-form expression for the MC, as an *explicit* function of the magnetic flux. From Eq. (49) it becomes evident that a magnetic field leads to an increase in the *positive* MC: $G(\phi)/G(0)$ increases from 1 to a saturated value 2 (since $S(2\phi)$ decreases from N to 0) when the flux is turned on and increased. $G(\phi) = 2G(0)$ at the field ϕ that satisfies $S(2\phi) = 0$. Furthermore, it is clear that the MC varies *periodically* with the magnetic field and the periodicity in the flux is equal to the superconducting flux quantum $hc/2e$.

It is important to point out that Eqs. (48) and (49) are valid in any dimension as long as we use the corresponding D-dimensional sum $S^{(r)}$.

It is illuminating to draw attention to the close relationship between the behaviors of $I_{2m}(2\phi) = S_{m,m}(2\phi)$ and the corresponding $G(\phi)$. When $\phi = 0$, $(I_{2m}(0)/N)^2 = 1$, which is the *largest* value of $(I_{2m}(2\phi)/N)^2$ as a function of ϕ , and the MC is equal to the *smallest* value $G(0)$. When the magnetic field is increased from zero, $(I_{2m}(2\phi)/N)^2$ quickly approaches (more rapidly as m becomes larger) its *smallest* value, which is zero, at $\phi/2\pi = 1/4m$. At the same time, the MC rapidly increases to the *largest* value $2G(0)$.

The physical implication of this is clear: fully constructive interference in the case without disorder leads to the smallest hopping conduction in the presence of disorder. While fully destructive interference in the case without disorder yields the largest hopping conduction in the presence of disorder. Moreover, when m (the system size is $m \times m$) is large, $G(\phi)/G(0)$ remains in the close vicinity of 2 for $\phi/2\pi > 1/4m$ in spite of the strong very-small-magnitude fluctuations of $I_{2m}(2\phi)/N$ around zero.

The saturated value of the magnetic field B_{sa} (i.e., the first field that makes $G(\phi) = 2G(0)$) is inversely proportional to twice the hopping length: the larger the system is, the smaller B_{sa} will be. In other words, as soon as the system, with hopping distance $r = 2m$, is penetrated by a total flux of $(1/2r) \times (r/2)^2 = r/8$ (in units of the flux quantum hc/e), the MC reaches the saturation value $2G(0)$.

Defining the relative MC, $\Delta G(\phi)$, as

$$\Delta G(\phi) \equiv \frac{G(\phi) - G(0)}{G(0)},$$

and utilizing Eq. (49), we show $\Delta G(\phi)$ versus ϕ for several different hopping lengths in Fig. 5. The behavior of $\Delta G(\phi)$ described above can be clearly observed in these figures.

Now let us examine the behavior of the MC in the low-flux limit. From Eqs. (14) and (15), it follows then that, for very small fields, in 2D

$$\Delta G(\phi) \simeq \frac{\sqrt{3}}{6} r^{3/2} \phi, \quad (50)$$

and in ladder-type quasi-1D structures

$$\Delta G(\phi) \simeq \frac{\sqrt{3}}{3} r \phi. \quad (51)$$

In Fig. 6, we plot $\Delta G(\phi)$ computed directly from Eq. (49), for various small values of ϕ , versus $r^{3/2}\phi$, with $r = 2, 4, \dots, 1000$, in (a) and versus $r\phi$, with $r = 2, 3, \dots, 500$, in (b), respectively for 2D and quasi-1D systems. It is seen that, both in (a) and (b), all the data nicely collapses into a straight line, which verifies the scaling of the low-flux MC in Eqs. (50) and (51).

If we consider the second leading terms in the moments, namely Eqs. (39) and (40), the second-order contribution to the L_{MC} is

$$L_{MC} = \begin{cases} 0 & \text{when } S(2\phi)/N = \pm 1 \\ \frac{1}{6N} \left\{ 1 - \sum_{k=1}^{\infty} \left[\frac{(2k+1)!}{(2^k k!)^2} \left(\frac{2k-3}{2k+1} - \frac{k}{k+1} \frac{S(4\phi)}{N} \right) \left(\frac{S(2\phi)}{N} \right)^{2k} \right] \right\} & \text{when } S(2\phi)/N \neq \pm 1 \\ 0 & \text{when } \Lambda = 0 \\ \frac{1}{6N} \left\{ 1 - \frac{1-\Lambda}{\Lambda^3(1+\Lambda)} \left[\left(1 - \frac{S(4\phi)}{N} \right) (1 + 2\Lambda) - \Lambda^2(2 + 3\Lambda) \right] \right\} & \text{when } \Lambda \neq 0 \end{cases}, \quad (52)$$

where

$$\Lambda = \sqrt{1 - \left(\frac{S(2\phi)}{N}\right)^2},$$

and we have used

$$\begin{aligned} \sum_{k=1}^{\infty} \frac{(2k)!}{(2^k k!)^2} x^{2k} &= \frac{1 - \sqrt{1 - x^2}}{\sqrt{1 - x^2}}, \\ \sum_{k=1}^{\infty} 2k \frac{(2k)!}{(2^k k!)^2} x^{2k} &= \frac{x^2}{(1 - x^2)^{3/2}}, \\ \sum_{k=1}^{\infty} \frac{(2k)!}{(k+1)(2^k k!)^2} x^{2k} &= \frac{x^2}{(1 - \sqrt{1 - x^2})^2}. \end{aligned}$$

The principal features in the behavior of the MC are not significantly modified by the addition of the contribution from L_{MC} in Eq. (52): while the magnitude of $\Delta G(\phi)$ is slightly increased for $\phi \neq 0$, the period of the MC remains unchanged.

For a 2D system and in the low-flux limit, we derive from Eq. (52) for diagonal sites $(r/2, r/2)$:

$$\Delta G(\phi) = (\sqrt{3}/24N) r^{3/2} \phi.$$

Comparing this result with Eq. (50), we see that the dependence of the small-field MC on the hopping length and the field is the same except for different prefactors. Summing up both contributions, we have for small ϕ

$$\Delta G(\phi) = \frac{\sqrt{3}}{6} \left(1 + \frac{1}{4N}\right) r^{3/2} \phi. \quad (53)$$

In addition, when $S(2p\phi) = 0$, we have from Eqs. (37-42)

$$L_{MC} = \ln 2 + \frac{1}{6N} + \frac{7}{60N^2} + O\left(\frac{1}{N^3}\right). \quad (54)$$

This indicates that the magnitude of the positive MC is gradually increased (e.g., the saturation value of ΔG is raised above 1) when contributions from higher-order terms (i.e., terms $\propto 1/N^k$ with $k \geq 1$) are included, though they are negligibly small.

D. Discussion

Our results for the MC are in good agreement with experimental measurements.^{19,20} For instance, a positive MC is observed in the VRH regime of both macroscopically large $\text{In}_2\text{O}_{3-x}$ samples¹⁹ and compensated n-type CdSe .²⁰ Moreover, saturation in the MC as the field is increased is also reported in Ref. 20.

The results for $\Delta G(\phi)$ presented in this work are consistent with theoretical studies based on an independent-directed-path formalism⁸ and a random matrix theory of the transition strengths.⁹ The advantages of our results include: (i) they provide explicit expressions for the first two dominant contribution to the MC, as a function of the magnetic field; (ii) they provide straightforward determination of the period of the oscillation of the MC; (iii) they provide explicit scaling behaviors (i.e., the dependence on the hopping length and the orientation and strength of the field) of the low-flux MC in quasi 1-D, 2D and 3D systems; and (iv) they allow us to make quantitative comparison with experimental data. Finally, it is important to emphasize that our analytic results [Eqs. (48), (49) and (52)] for the MC are equally applicable to *any dimension*, since the essential ingredient in our expressions is the QI quantity $S^{(r)}$, which takes into account the dimensionality.

In appendix B, we outline the computational scheme using the second model of disorder, i.e., ϵ_i is randomly chosen from the interval $[-W/2, W/2]$. The moments obtained in this case are the same as those presented in Eqs. (37) and (38). Therefore, the result for the MC remains unchanged.

IV. QUANTUM INTERFERENCE AND THE SMALL-FIELD MAGNETOCONDUCTANCE ON A THREE-DIMENSIONAL CUBIC LATTICE

A. Sums over forward-scattering paths

Let $\mathcal{S}_{m,n,l}$ ($= S^{(r)}$ in 3D) be the sum over all phase factors associated with directed paths of $m+n+l$ ($= r$) steps along which an electron may hop from $(0,0,0)$ to the site (m,n,l) . Again we assume m, n , and $l \geq 0$. In other words, electrons can now also hop in the positive z direction. The vector potential of a general magnetic field (B_x, B_y, B_z) can be written as

$$\mathbf{A} = \frac{1}{2}(zB_y - yB_z, xB_z - zB_x, yB_x - xB_y).$$

Also, $a/2\pi$, $b/2\pi$ and $c/2\pi$ represent the three fluxes through the respective elementary plaquettes on the yz -, zx - and xy -planes. To compute $\mathcal{S}_{m,n,l}$, we start from the following recursion relation

$$\mathcal{S}_{m,n,l} = \sum_{p=0}^m \sum_{q=0}^n A_{p,q,l \rightarrow m,n,l} \exp\left(i \frac{qa - pb}{2}\right) \mathcal{S}_{p,q,l-1}, \quad (55)$$

where $A_{p,q,l \rightarrow m,n,l}$ is the sum over all directed paths starting from (p,q,l) and ending at (m,n,l) . The physical meaning of Eq. (55) is as follows. The site (m,n,l) is reached by taking one step from $(p,q,l-1)$ to (p,q,l) , acquiring the phase $i(qa - pb)/2$, then traversing from (p,q,l) to (m,n,l) on the $z = l$ plane. After some calculation, we find that

$$A_{p,q,l \rightarrow m,n,l} = \exp\left\{i \left[\frac{(m-p)(lb - qc) + (n-q)(pc - la)}{2} \right]\right\} \mathcal{S}_{m-p,n-q}(c), \quad (56)$$

where $\mathcal{S}_{m-p,n-q}(c)$ is defined as shown in Eq. (10). By applying Eq. (56) l times, we obtain a general formula of $\mathcal{S}_{m,n,l}$ for $m, n, l \geq 1$ in terms of the fluxes a, b and c as

$$\mathcal{S}_{m,n,l}(a, b, c) = \exp\left[-i \left(\frac{nla + lmb + mnc}{2} \right)\right] \mathcal{L}_{m,n,l}(a, b, c), \quad (57)$$

where

$$\mathcal{L}_{m,n,l}(a, b, c) = \left\{ \prod_{j=1}^l \left[\sum_{p_j=0}^{p_{j+1}} \sum_{q_j=0}^{q_{j+1}} \exp\{i[q_j a + (m-p_j)b + p_j(q_{j+1} - q_j)c]\} L_{p_{j+1}-p_j, q_{j+1}-q_j}(c) \right] \right\} L_{p_1, q_1}(c), \quad (58)$$

with $p_{l+1} \equiv m$, $q_{l+1} \equiv n$, and the $L_{p,q}(c)$'s are defined as in Eq. (12).

It is clear that $\mathcal{S}_{m,n,0} = \mathcal{S}_{m,n}(c)$, $\mathcal{S}_{m,0,l} = \mathcal{S}_{m,l}(b)$, and $\mathcal{S}_{0,n,l} = \mathcal{S}_{n,l}(a)$. Also, the following symmetries hold:

$$\mathcal{S}_{m,n,l}(a, b, c) = \mathcal{S}_{n,m,l}(b, a, c) = \mathcal{S}_{m,l,n}(a, c, b) = \mathcal{S}_{l,m,n}(b, c, a) = \mathcal{S}_{l,n,m}(c, b, a) = \mathcal{S}_{n,l,m}(c, a, b). \quad (59)$$

When there is no magnetic flux,

$$\mathcal{S}_{m,n,l}(0, 0, 0) = \frac{(m+n+l)!}{m!n!l!} \equiv \mathcal{N}$$

gives the total number of $(m+n+l)$ -step paths connecting $(0,0,0)$ and (m,n,l) .

We have obtained explicit expressions for many $\mathcal{S}_{m,n,l}$, and here we explicitly present only the first few \mathcal{S} , since \mathcal{S} have long expressions for larger m, n , and l .

$$\begin{aligned} \mathcal{S}_{1,1,1} &= 2 \left[\cos \frac{a+b-c}{2} + \cos \frac{b+c-a}{2} + \cos \frac{c+a-b}{2} \right], \\ \mathcal{S}_{2,1,1} &= 2 \left[\cos \frac{a}{2} + \cos \left(\frac{a}{2} - b \right) + \cos \left(\frac{a}{2} - c \right) + \cos \left(\frac{a}{2} \pm b \mp c \right) + \cos \left(\frac{a}{2} - b - c \right) \right], \\ \mathcal{S}_{2,2,1} &= 2 + 2 \sum^{(1)} \cos \alpha + 4 \cos(a-b) + 2 \cos(a-c) + 2 \cos(b-c) + 2 \cos(a-2c) + 2 \cos(b-2c) \\ &\quad + 2 \cos(a-b \pm c) + 2 \cos(a+b-2c) + 2 \cos(a-b \pm 2c), \\ \mathcal{S}_{2,2,2} &= 6 + \sum^{(1)} [4 \cos \alpha + 2 \cos 2\alpha] + \sum^{(2)} [4 \cos(\alpha - \beta) + 4 \cos 2(\alpha - \beta) + 2 \cos(\alpha - 2\beta) + 2 \cos(2\alpha - \beta)] \\ &\quad + 2 \sum^{(3)} [\cos(\alpha + \beta - \gamma) + \cos 2(\alpha + \beta - \gamma) + \cos(\alpha + \beta - 2\gamma) + \cos(\alpha \pm 2\beta \mp 2\gamma)]. \end{aligned}$$

Here $\sum^{(i)}$ denote sums over $\alpha = a, b, c$; $(\alpha\beta) = (ab), (bc), (ca)$; and $(\alpha\beta\gamma) = (abc), (bca), (cab)$; for $i = 1, 2$, and 3 respectively; and, for instance, the term $\cos(a/2 \pm b \mp c)$ means $\cos(a/2 + b - c) + \cos(a/2 - b + c)$.

B. Low-flux limit

In the very-low-flux limit, and calculated exactly to second-order in the flux, we obtain the logarithm of $\mathcal{S}_{m,n,l}$, the 3D analog of the harmonic shrinkage of the wave function, as

$$\ln \mathcal{S}_{m,n,l} = \ln \mathcal{N} - \frac{1}{24} [nla^2 + lmb^2 + mnc^2 + m(lb - nc)^2 + n(mc - la)^2 + l(na - mb)^2]. \quad (60)$$

This generalizes the 2D harmonic-shrinkage of the wave function obtained in Eq. (13). When $m = n = l = r/3$, we have

$$\ln \mathcal{S}_{m,m,m} = \ln \frac{r!}{[(r/3)!]^3} - \frac{1}{216} \left\{ r^2(a^2 + b^2 + c^2) + \frac{r^3}{3} [(b-c)^2 + (c-a)^2 + (a-b)^2] \right\}. \quad (61)$$

These results generalize to 3D the 2D results obtained in Sec. II B.

C. Interference patterns on diagonal sites

In order to see how the interference patterns vary according to the orientation of the applied field, we focus on $\mathcal{S}_{m,m,m}$ (i.e., \mathcal{S} on the body diagonals). We now examine two special cases: $\mathbf{B}_{\parallel} \equiv \mathbf{B} \parallel (1, 1, 1) = (\phi, \phi, \phi)/2\pi$ and $\mathbf{B}_{\perp} \equiv \mathbf{B} \perp (1, 1, 1) = (\phi/2, \phi/2, -\phi)/2\pi$, namely fields parallel and perpendicular to the $(1, 1, 1)$ direction, respectively. Their $\mathcal{S}_{m,m,m}$'s are denoted respectively by $\mathcal{I}_{3m}^{\parallel}$ and \mathcal{I}_{3m}^{\perp} and have been computed to high orders. Here we only present the first few:

$$\begin{aligned} \mathcal{I}_3^{\parallel} &= 6 \cos \theta, \\ \mathcal{I}_6^{\parallel} &= 36 + 42 \cos 2\theta + 12 \cos 4\theta, \\ \mathcal{I}_9^{\parallel} &= 864 \cos \theta + 528 \cos 3\theta + 216 \cos 5\theta + 54 \cos 7\theta + 18 \cos 9\theta, \\ \mathcal{I}_{12}^{\parallel} &= 7308 + 12504 \cos 2\theta + 8082 \cos 4\theta + 4032 \cos 6\theta + 1740 \cos 8\theta \\ &\quad + 672 \cos 10\theta + 216 \cos 12\theta + 72 \cos 14\theta + 24 \cos 16\theta; \end{aligned}$$

and

$$\begin{aligned} \mathcal{I}_3^{\perp} &= 4 \cos \theta + 2 \cos 2\theta, \\ \mathcal{I}_6^{\perp} &= 14 + 12 \cos \theta + 16 \cos 2\theta + 12 \cos 3\theta + 12 \cos 4\theta + 8 \cos 5\theta + 10 \cos 6\theta + 4 \cos 7\theta + 2 \cos 8\theta, \\ \mathcal{I}_9^{\perp} &= 76 + 204 \cos \theta + 176 \cos 2\theta + 180 \cos 3\theta + 156 \cos 4\theta + 156 \cos 5\theta + 136 \cos 6\theta \\ &\quad + 128 \cos 7\theta + 102 \cos 8\theta + 84 \cos 9\theta + 68 \cos 10\theta + 64 \cos 11\theta + 48 \cos 12\theta \\ &\quad + 40 \cos 13\theta + 26 \cos 14\theta + 20 \cos 15\theta + 10 \cos 16\theta + 4 \cos 17\theta + 2 \cos 18\theta, \\ \mathcal{I}_{12}^{\perp} &= 1372 + 2464 \cos \theta + 2606 \cos 2\theta + 2420 \cos 3\theta + 2502 \cos 4\theta + 2288 \cos 5\theta + 2288 \cos 6\theta + 2068 \cos 7\theta \\ &\quad + 2046 \cos 8\theta + 1788 \cos 9\theta + 1758 \cos 10\theta + 1532 \cos 11\theta + 1498 \cos 12\theta + 1264 \cos 13\theta \\ &\quad + 1174 \cos 14\theta + 964 \cos 15\theta + 894 \cos 16\theta + 724 \cos 17\theta + 642 \cos 18\theta + 512 \cos 19\theta \\ &\quad + 450 \cos 20\theta + 340 \cos 21\theta + 296 \cos 22\theta + 228 \cos 23\theta + 178 \cos 24\theta + 128 \cos 25\theta \\ &\quad + 94 \cos 26\theta + 56 \cos 27\theta + 40 \cos 28\theta + 20 \cos 29\theta + 10 \cos 30\theta + 4 \cos 31\theta + 2 \cos 32\theta. \end{aligned}$$

where $\theta = \phi/2$. It can be seen that $\mathcal{I}_{3m}^{\parallel}$ and \mathcal{I}_{3m}^{\perp} exhibit quite different behaviors as shown in Fig. 7 where we plot $\mathcal{I}_3^{\parallel}$ through $\mathcal{I}_{12}^{\parallel}$ and \mathcal{I}_3^{\perp} through \mathcal{I}_{12}^{\perp} . Notice that the period in ϕ for $\mathcal{I}_{3m}^{\parallel}$ is 2π (4π) for even (odd) m , while the period for \mathcal{I}_{3m}^{\perp} is 4π for any m . Therefore, the periodicity for the MC in 3D is identical to that in 2D.

We have also computed $\mathcal{I}_{3m}^{\parallel}$ and \mathcal{I}_{3m}^{\perp} ($m = 1, 2, \dots, 300$) for $\phi/2\pi = 3/5$ and $(\sqrt{5} - 1)/2$ and find that their behaviors are insensitive to the commensurability of ϕ , unlike the case on a square lattice. Physically, this can be understood because two randomly chosen paths have a higher probability of crossing (and thus interfering) in 2D than in 3D; thus making QI effects less pronounced in 3D than in 2D. A similar situation occurs classically (e.g., multiply-scattered light in a random medium^{15,16}).

D. Small-field magnetoconductance

For a 3D system, the relative MC, $\Delta G(a, b, c)$, now reads

$$\Delta G(a, b, c) = \sqrt{1 - \left[\frac{\mathcal{S}_{m,n,l}(2a, 2b, 2c)}{\mathcal{N}} \right]^2}. \quad (62)$$

The above general expression is valid for any ending site as well as arbitrary orientation and strength of the magnetic field. From Eq. (61), in the small-field limit and at ending site $(r/3, r/3, r/3)$, we have

$$\Delta G = \frac{1}{3\sqrt{3}} \sqrt{r^2(a^2 + b^2 + c^2) + \frac{r^3}{3} [(b-c)^2 + (c-a)^2 + (a-b)^2]}, \quad (63)$$

which is applicable for any orientation of the field. Below we focus on two special orientations of the field: \mathbf{B}_\perp and \mathbf{B}_\parallel .

For very small ϕ , we have from Eq. (61)

$$\ln \mathcal{I}_r^\perp \simeq \ln \frac{r!}{[(r/3)!]^3} - \frac{1}{144} r^2 (r+1) \phi^2, \quad (64)$$

and

$$\ln \mathcal{I}_r^\parallel \simeq \ln \frac{r!}{[(r/3)!]^3} - \frac{1}{72} r^2 \phi^2. \quad (65)$$

The 3D behavior of the low-flux MC thus becomes clear: for \mathbf{B}_\perp

$$\Delta G(\phi) \simeq \frac{\sqrt{2}}{6} r^{3/2} \phi, \quad (66)$$

and for \mathbf{B}_\parallel

$$\Delta G(\phi) \simeq \frac{1}{3} r \phi. \quad (67)$$

These results can be interpreted as follows: the effective area A_\perp^{eff} exposed to \mathbf{B}_\perp is larger,

$$A_\perp^{\text{eff}} \sim r^{3/2},$$

similar to the 2D case where $\Delta G(\phi) \propto r^{3/2} \phi$; while the effective area A_\parallel^{eff} exposed to \mathbf{B}_\parallel is smaller,

$$A_\parallel^{\text{eff}} \sim r,$$

thus closer to our quasi-1D ladder case with $\Delta G(\phi) \propto r \phi$.

As a numerical test of Eqs. (66) and (67), in Fig. 8 we show ΔG calculated directly from Eq. (62), versus $r^{3/2}\phi$ in (a) and versus $r\phi$ in (b), respectively for several values of \mathbf{B}_\perp and \mathbf{B}_\parallel with hopping length $r = 3, 6, \dots, 600$. The collapse of all the data into a straight line verifies the scaling of the low-flux ΔG presented above.

E. Average of the magnetoconductance over angles

In a macroscopic sample, the conductance may be determined by *a few* (instead of one, as considered before) critical hopping events. As a result of this, the observed MC of the whole sample should be the average of the MC associated with these critical hops. Thus, in 3D systems it is also important to take into account the randomness of the angles between the hopping direction and the orientation of the applied magnetic field.²¹

To theoretically investigate the effect of the average over angles on the MC, we consider all possible relative hopping directions with respect to that of the magnetic field, or equivalently, the continuously-varying orientation of the field with respect to a fixed hopping direction. We adopt the latter below: the ending site of all hopping events (with the same hopping length r) is located at the diagonal point $(r/3, r/3, r/3)$ and the magnetic field can be adjusted

between the parallel and perpendicular directions with respect to the vector $\mathbf{d} = (1, 1, 1)$. Our interest here is in the MC averaged over angles, denoted by $\overline{\Delta G}$, in the low-field limit. Recall that the magnetic field is $\mathbf{B} = (a, b, c)/2\pi$, and from Eq. (63), we have

$$\Delta G = \frac{2\pi}{3\sqrt{3}} r B \sqrt{1 + r \sin^2 \omega}, \quad (68)$$

where $B = \sqrt{a^2 + b^2 + c^2}/2\pi$ is the magnitude of the field and ω is the angle between \mathbf{B} and \mathbf{d} . By averaging over the angle ω , we obtain

$$\begin{aligned} \overline{\Delta G}(B) &= \frac{4}{3\sqrt{3}} r B \int_0^{\pi/2} \sqrt{1 + r \sin^2 \omega} d\omega \\ &= \frac{4}{3\sqrt{3}} r \sqrt{r+1} B E\left(\frac{\pi}{2}, \frac{\sqrt{r}}{\sqrt{r+1}}\right), \end{aligned} \quad (69)$$

where $E(\pi/2, \sqrt{r}/\sqrt{r+1})$ is the complete elliptic integral of the second kind. When r is large, $E(\pi/2, \sqrt{r}/\sqrt{r+1}) \simeq 1$ and we therefore have

$$\overline{\Delta G}(B) \simeq \frac{4}{3\sqrt{3}} r^{3/2} B. \quad (70)$$

Equation (70) means that the dominant contribution to the MC stems from the critical hop which is *perpendicular* to the field. This is understandable through our earlier observation that the effective area enclosed by the electron is largest when \mathbf{B} is perpendicular to \mathbf{d} . From the above analysis, we conclude that in 3D macroscopic samples the low-field MC should in principle behave as $r^{3/2} B$.

V. CONCLUDING REMARKS AND SUMMARY OF RESULTS

In closing we briefly address four issues. First, although relevant measurable quantities such as $|S_{m,n}|^2$ and $|S_{m,n,l}|^2$ are gauge-invariant, the transition amplitudes are gauge dependent. As an illustration, the transition amplitude will be $L_{m,n}$ [Eq. (12)] if we use the Landau gauge $\mathbf{A} = (0, Bx)$ on a square lattice. The notation $S_{m,n}$ ($L_{m,n}$) refers the use of the Symmetric (Landau) gauge. Similarly, the transition amplitude will read $\mathcal{L}_{m,n,l}$ [Eq. (58)] if we use the gauge $\mathbf{A} = (B_y z, B_z x, B_x y)$ on a cubic lattice.

Second, returns to the origin (see, e.g., Refs. 1 and 22-24) become important for less strongly localized electrons, and their QI effects^{22,23} can be incorporated in our approach.

Third, the main limitations of our study in the case with impurities are the following: no inclusion of spin-orbit scattering effects (for this see, e.g., Refs. 7-9 and references therein), and no explicit inclusion of the correlations between crossing paths, as discussed in Refs. 4 and 7. However, these correlations are negligible when spin-orbit scattering is present.⁷

Fourth, besides analytical closed-form results in 2D, this work presents exact results for 3D systems, e.g., $\Delta G = (2\pi/3\sqrt{3})rB(1 + r \sin^2 \omega)^{1/2}$ [Eq. (68)]. These results can provide further tests of the quantum interference effects. This can be done by measuring the MC of bulk samples (which are small enough that only a single critical hop is allowed) in various orientations of the field. By doing this, one can then *determine* the values of r and ω (and, hence, also the direction of this critical hop). Therefore, the small-field behaviors of the MC with fields parallel and perpendicular to the direction of this critical hop can be measured and compared to our predictions. This could potentially be very useful.

In summary, we present an investigation of quantum interference phenomena and the magnetic-field effects on the MC resulting from sums over directed paths on resistor networks in 2D and 3D. The principal results include: (1) an exact and explicit closed-form expression for the sum over forward-scattering paths $S^{(r)}$ to any site on a square lattice, which is the essential QI quantity in both uniform and disordered cases, (2) an explicit formula for $S^{(r)}$ for electrons hopping on a cubic lattice, (3) the low-flux behaviors of $S^{(r)}$ in both 2D and 3D, (4) the exact summation of the dominant winding paths in 2D, (5) compact, analytic results for the positive MC as explicit functions of the magnetic flux which are valid in any dimension, (6) the small-field behaviors of the MC in quasi-1D, 2D and 3D, and (7) an analytic result for the small-field MC in 3D incorporating the randomness in the relative angles between the hops and the applied field. They provide analytical and explicit closed-form results concerning the hopping transport of strongly localized electrons subject to an external magnetic field in the macroscopic regime. We hope that our results stimulate further work (e.g., inclusion of spin-orbit effects on lattice path integrals) on exact results in 2D and 3D systems.

ACKNOWLEDGMENTS

It is a great pleasure to thank B.L. Altshuler, M. Kardar, E. Medina, Y. Meir, Y. Shapir and J. Stemberge for their very useful suggestions. F.N. acknowledges partial support from the UCSB Institute for Theoretical Physics through the NSF grant No. PHY89-04035, the NATO office of Scientific Affairs, and the Office of the Vice Provost for Academic and Multicultural Affairs, through a Faculty Career Development Award during the Fall of 1994.

APPENDIX A: DERIVATION OF THE MOMENTS $\langle J_{M,N}^{2P}(\phi) \rangle$ AND $\langle |J_{M,N}(\phi)|^{2P} \rangle$

In this appendix, we outline the derivation of the moments shown in Eqs. (32), (33), (35), and (36). First, let us derive Eqs. (32) and (33). Let $s_i = \exp(i\Phi_i)$, where Φ_i is the sum over all phases along path i and $i = 1, 2, \dots, N$. Note that for *every* path, the probability for obtaining the overall phase factor $\pm s_i$ is P_{\pm} . Now

$$J^2 = \left(\sum_{i=1}^N \gamma_i s_i \right) \left(\sum_{i=1}^N \gamma_i s_i \right)$$

and

$$|J|^2 = \left(\sum_{i=1}^N \gamma_i s_i \right) \left(\sum_{i=1}^N \gamma_i \frac{1}{s_i} \right),$$

where $\gamma_i = \pm 1$ with probability P_{\pm} . If the number of $\gamma_i = -1$ is k , the overall probability is $P_+^{N-k} P_-^k$ and there are C_k^N combinations among γ_i ($i = 1, \dots, N$). For $k = 0$ and $k = N$, there is only one combination producing $S(2\phi) + 2 \sum_{i \neq j} s_i s_j$ for J^2 and also only one combination producing $N + \sum_{i \neq j} s_i/s_j$ for $|J|^2$. When $1 \leq k \leq N - 1$, for J^2 there are $N_- = 2 C_{k-1}^{N-2}$ combinations producing $S(2\phi) - 2 \sum_{i \neq j} s_i s_j$ and $N_+ = C_k^N - 2 C_{k-1}^{N-2}$ combinations producing $S(2\phi) + 2 \sum_{i \neq j} s_i s_j$. Also, when $1 \leq k \leq N - 1$, for $|J|^2$ there are N_- combinations producing $N - \sum_{i \neq j} s_i/s_j$ and N_+ combinations producing $N + \sum_{i \neq j} s_i/s_j$. In N_- , the factor 2 comes from the two possible ways: $+s_i - s_j$ and $-s_i + s_j$. C_{k-1}^{N-2} comes from arranging $(k-1)$'s minus signs among the $(N-2)$ s_l 's left ($l \neq i \neq j$). Therefore, the overall average is $\mathcal{P} = P_+^N + P_-^N + \sum_{k=1}^{N-1} (N_+ - N_-) P_+^{N-k} P_-^k = (\mu - \nu)^{2r}$. We thus have

$$\langle J^2 \rangle = S(2\phi) + \mathcal{P} \left(2 \sum_{i \neq j} s_i s_j \right),$$

where we have used the relation $\sum_{k=0}^N C_k^N P_+^{N-k} P_-^k = (P_+ + P_-)^N = 1$. Similarly,

$$\langle |J|^2 \rangle = N + \mathcal{P} \sum_{i \neq j} \frac{s_i}{s_j}.$$

By exploiting

$$2 \sum_{i \neq j} s_i s_j = S^2(\phi) - S(2\phi)$$

and

$$\sum_{i \neq j} \frac{s_i}{s_j} = S^2(\phi) - N,$$

we thus obtain Eqs. (32) and (33).

For $\mu = \nu = 1/2$, (namely, each site contributes either $+1$ or -1 with equal probability), $P_{\pm} = 1/2$ for *every* path i . The total number of sites that can be visited is $T = (m+1)(n+1) - 1$ (the initial site is not counted). Therefore, the total number of all possible impurity configurations is 2^T . Let us now focus on the $\gamma_i s_i$ with $i = 1, 2, \dots, N$. The total number of configuration sets is 2^N since each γ_i can be either $+1$ or -1 with equal probability. Among the 2^T impurity configurations, there are *always* $2^T/2^N$ producing a set of $\gamma_i s_i$ for *every* possible set of $\gamma_i s_i$. For instance,

$T = 3$ and $N = 2$ in the simplest case $S_{1,1}$. Among $2^3 = 8$ impurity configurations, two of them give $+s_1 + s_2$, $+s_1 - s_2$, $-s_1 + s_2$, and $-s_1 - s_2$. We thus have

$$\langle J^{2p} \rangle = \frac{1}{2^N} \sum_{\{\gamma_i\}} \left[\left(\sum_{i=1}^N \gamma_i s_i \right)^p \left(\sum_{i=1}^N \gamma_i s_i \right)^p \right],$$

and similarly,

$$\langle |J|^{2p} \rangle = \frac{1}{2^N} \sum_{\{\gamma_i\}} \left[\left(\sum_{i=1}^N \gamma_i s_i \right)^p \left(\sum_{i=1}^N \gamma_i \frac{1}{s_i} \right)^p \right].$$

The summation in $\{\gamma_i\}$ is over all possible configuration sets of γ_i . In other words, the average of A over disorder (i.e., $\langle A \rangle$) means to sum over all possible $\gamma_i = \pm 1$ for the desired quantity A , and then divide the sum by 2^N . We thus obtain

$$\begin{aligned} \langle J^4 \rangle &= S(4\phi) + \frac{4!}{(2!)^2} \sum_{i \neq j} s_i^2 s_j^2, \\ \langle J^6 \rangle &= S(6\phi) + \frac{6!}{4!2!} \sum_{i \neq j} s_i^4 s_j^2 + \frac{6!}{(2!)^3} \sum_{i \neq j \neq k} s_i^2 s_j^2 s_k^2, \\ \langle J^8 \rangle &= S(8\phi) + \frac{8!}{6!2!} \sum_{i \neq j} s_i^6 s_j^2 + \frac{8!}{(4!)^2} \sum_{i \neq j} s_i^4 s_j^4 + \frac{8!}{4!(2!)^2} \sum_{i \neq j \neq k} s_i^4 s_j^2 s_k^2 + \frac{8!}{(2!)^4} \sum_{i \neq j \neq k \neq l} s_i^2 s_j^2 s_k^2 s_l^2, \\ \langle J^{10} \rangle &= S(10\phi) + \frac{10!}{8!2!} \sum_{i \neq j} s_i^8 s_j^2 + \frac{10!}{6!4!} \sum_{i \neq j} s_i^6 s_j^4 + \frac{10!}{6!(2!)^2} \sum_{i \neq j \neq k} s_i^6 s_j^2 s_k^2 + \frac{10!}{(4!)^2 2!} \sum_{i \neq j \neq k} s_i^4 s_j^4 s_k^2 \\ &\quad + \frac{10!}{4!(2!)^3} \sum_{i \neq j \neq k \neq l} s_i^4 s_j^2 s_k^2 s_l^2 + \frac{10!}{(2!)^5} \sum_{i \neq j \neq k \neq l \neq m} s_i^2 s_j^2 s_k^2 s_l^2 s_m^2; \end{aligned}$$

and

$$\begin{aligned} \langle |J|^4 \rangle &= N(2N-1) + \sum_{i \neq j} \frac{s_i^2}{s_j^2}, \\ \langle |J|^6 \rangle &= N(6N^2 - 9N + 4) + 3(3N-4) \sum_{i \neq j} \frac{s_i^2}{s_j^2}, \\ \langle |J|^8 \rangle &= N(24N^3 - 72N^2 + 82N - 33) + 4(18N^2 - 57N + 49) \sum_{i \neq j} \frac{s_i^2}{s_j^2} + \sum_{i \neq j} \frac{s_i^4}{s_j^4} \\ &\quad + 6 \sum_{i \neq j \neq k} \left(\frac{s_i^4}{s_j^2 s_k^2} + \frac{s_j^2 s_k^2}{s_i^4} \right) + \sum_{i \neq j \neq k \neq l} \frac{s_k^2 s_l^2}{s_i^2 s_j^2}, \\ \langle |J|^{10} \rangle &= N(120N^4 - 600N^3 + 1250N^2 - 1225N + 456) + 20(30N^3 - 165N^2 + 325N - 224) \sum_{i \neq j} \frac{s_i^2}{s_j^2} \\ &\quad + 5(5N-8) \sum_{i \neq j} \frac{s_i^4}{s_j^4} + 10(15N-32) \sum_{i \neq j \neq k} \left(\frac{s_i^4}{s_j^2 s_k^2} + \frac{s_j^2 s_k^2}{s_i^4} \right) + 300(3N-8) \sum_{i \neq j \neq k \neq l} \frac{s_i^2 s_j^2}{s_k^2 s_l^2}. \end{aligned}$$

Noticing that $\sum_{i=1}^N s_i^m = \sum_{i=1}^N 1/s_i^m = S(m\phi)$, it can be derived that:

$$\begin{aligned} \sum_{i \neq j} s_i^2 s_j^2 &= \frac{1}{2} [S^2(2\phi) - S(4\phi)], \\ \sum_{i \neq j} s_i^4 s_j^2 &= S(2\phi) S(4\phi) - S(6\phi), \end{aligned}$$

$$\begin{aligned}
\sum_{i \neq j} s_i^4 s_j^4 &= \frac{1}{2} [S^2(4\phi) - S(8\phi)], \\
\sum_{i \neq j} s_i^6 s_j^2 &= S(2\phi) S(6\phi) - S(8\phi), \\
\sum_{i \neq j} s_i^8 s_j^2 &= S(2\phi) S(8\phi) - S(10\phi), \\
\sum_{i \neq j} s_i^6 s_j^4 &= S(4\phi) S(6\phi) - S(10\phi), \\
\sum_{i \neq j \neq k} s_i^2 s_j^2 s_k^2 &= \frac{1}{6} S^3(2\phi) - \frac{1}{2} S(2\phi) S(4\phi) + \frac{1}{3} S(6\phi), \\
\sum_{i \neq j \neq k} s_i^4 s_j^2 s_k^2 &= \frac{1}{2} S^2(2\phi) S(4\phi) - S(2\phi) S(6\phi) - \frac{1}{2} S^2(4\phi) + S(8\phi), \\
\sum_{i \neq j \neq k} s_i^6 s_j^2 s_k^2 &= \frac{1}{2} S^2(2\phi) S(6\phi) - S(2\phi) S(8\phi) - \frac{1}{2} S(4\phi) S(6\phi) + S(10\phi), \\
\sum_{i \neq j \neq k} s_i^4 s_j^4 s_k^2 &= \frac{1}{2} S(2\phi) S^2(4\phi) - \frac{1}{2} S(2\phi) S(8\phi) - S(4\phi) S(6\phi) + S(10\phi), \\
\sum_{i \neq j \neq k \neq l} s_i^2 s_j^2 s_k^2 s_l^2 &= \frac{1}{24} S^4(2\phi) - \frac{1}{4} S^2(2\phi) S(4\phi) + \frac{1}{3} S(2\phi) S(6\phi) + \frac{1}{8} S^2(4\phi) - \frac{1}{4} S(8\phi), \\
\sum_{i \neq j \neq k \neq l} s_i^4 s_j^2 s_k^2 s_l^2 &= \frac{1}{6} S^3(2\phi) S(4\phi) - \frac{1}{2} S^2(2\phi) S(6\phi) - \frac{1}{2} S(2\phi) S^2(4\phi), \\
&\quad + S(2\phi) S(8\phi) + \frac{5}{6} S(4\phi) S(6\phi) - S(10\phi), \\
\sum_{i \neq j \neq k \neq l \neq m} s_i^2 s_j^2 s_k^2 s_l^2 s_m^2 &= \frac{1}{120} S^5(2\phi) - \frac{1}{12} S^3(2\phi) S(4\phi) + \frac{1}{6} S^2(2\phi) S(6\phi) + \frac{1}{8} S(2\phi) S^2(4\phi) \\
&\quad - \frac{1}{4} S(2\phi) S(8\phi) - \frac{1}{6} S(4\phi) S(6\phi) + \frac{1}{5} S(10\phi), \\
\sum_{i \neq j} \frac{s_i^2}{s_j^2} &= S^2(2\phi) - N, \\
\sum_{i \neq j} \frac{s_i^4}{s_j^4} &= S^2(4\phi) - N, \\
\sum_{i \neq j \neq k} \frac{s_i^4}{s_j^2 s_k^2} &= \sum_{i \neq j \neq k} \frac{s_j^2 s_k^2}{s_i^4} = \frac{1}{2} S^2(2\phi) S(4\phi) - S^2(2\phi) - \frac{1}{2} S^2(4\phi) + N, \\
\sum_{i \neq j \neq k \neq l} \frac{s_i^2 s_j^2}{s_k^2 s_l^2} &= \frac{1}{4} S^4(2\phi) - (N-2) S^2(2\phi) - \frac{1}{2} S^2(2\phi) S(4\phi) + \frac{1}{4} S^2(4\phi) + \frac{1}{2} N(N-3).
\end{aligned}$$

By utilizing the above relations, we have obtained the results for the moments presented in Eqs. (35.1)-(35.4) and (36.1)-(36.4).

APPENDIX B: A DIFFERENT MODEL OF DISORDER

In this appendix, we study another model of diagonal disorder: ϵ_i uniformly distributed between $-W/2$ and $W/2$. Our focus is on the analytical computation of the leading terms (terms $\propto N^p$) in the moments $\langle |J(0)|^{2p} \rangle$ and $\langle |J(\phi)|^{2p} \rangle$. Indeed, the scheme presented below applies equally to our first model of disorder, where ϵ_i can take two values, $+W$ and $-W$, with equal probability.

Let us write

$$J(\phi) = \sum_{i=1}^N \eta_i s_i,$$

where for each path i

$$\eta_i = \prod_{j=1}^r \left(-\frac{W}{\epsilon_j} \right).$$

It is reasonable to choose η_i from a Gaussian distribution of zero mean and unit standard deviation. We therefore have $\langle \eta_i^{2n} \rangle = 1$ and $\langle \eta_i^{2n+1} \rangle = 0$. For $\phi = 0$, we have

$$|J(0)|^{2p} = \left(\sum_{i=1}^N \eta_i \right)^{2p} = \prod_{k=1}^{2p} \left(\sum_{i_k=1}^N \eta_{i_k} \right).$$

It is found that the leading term in $\langle |J(0)|^{2p} \rangle$ comes from all terms having the form $\prod_{i=1}^p \eta_i^2$ and there are C_p^N distinct terms of this type, each term has a coefficient $(2p)!/2^p$. Therefore, we obtain for the leading term

$$\langle |J(0)|^{2p} \rangle = \frac{(2p)!}{2^p} \frac{N^p}{p!} = (2p-1)!! N^p.$$

For $\phi \neq 0$, we have now

$$\begin{aligned} |J(\phi)|^{2p} &= \left(\sum_{i=1}^N \eta_i s_i \right)^p \left(\sum_{i=1}^N \eta_i \frac{1}{s_i} \right)^p \\ &= \prod_{k=1}^p \left[\left(\sum_{i_k=1}^N \eta_{i_k} s_{i_k} \right) \left(\sum_{i'_k=1}^N \eta_{i'_k} \frac{1}{s_{i'_k}} \right) \right]. \end{aligned}$$

The contributions to the leading terms involve different factors, as shown below. There are C_p^N terms like

$$\left(\prod_{i=1}^p \eta_i s_i \right) \left(\prod_{i=1}^p \eta_i \frac{1}{s_i} \right),$$

and they contribute

$$(p!)^2 \frac{N^p}{p!} = p! N^p.$$

There are C_{p-2}^{N-2} terms like

$$\left(\eta_1^2 s_1^2 \prod_{i=2}^{p-1} \eta_i s_i \right) \left(\eta_{1'}^2 \frac{1}{s_{1'}^2} \prod_{i=2}^{p-1} \eta_i \frac{1}{s_i} \right),$$

and they contribute

$$\left(\frac{p!}{2} \right)^2 \frac{N^{p-2}}{(p-2)!} \frac{S^2(2\phi)}{(1!)^2} = p! \frac{2! C_2^p}{(2 \cdot 1!)^2} N^{p-2} S^2(2\phi).$$

Similarly, there are C_{p-4}^{N-4} terms like

$$\left(\eta_1^2 s_1^2 \eta_2^2 s_2^2 \prod_{i=3}^{p-2} \eta_i s_i \right) \left(\eta_{1'}^2 \frac{1}{s_{1'}^2} \eta_{2'}^2 \frac{1}{s_{2'}^2} \prod_{i=3}^{p-2} \eta_i \frac{1}{s_i} \right),$$

and they contribute

$$\left(\frac{p!}{2^2}\right)^2 \frac{N^{p-4}}{(p-4)!} \frac{S^4(2\phi)}{(2!)^2} = p! \frac{4! C_4^p}{(2^2 \cdot 2!)^2} N^{p-4} S^4(2\phi).$$

In general, there are C_{p-2k}^{N-2k} terms of the following type

$$\left(\prod_{i=1}^k \eta_i^2 s_i^2 \prod_{i=k+1}^{p-k} \eta_i s_i\right) \left(\prod_{i=1}^k \eta_{i'}^2 \frac{1}{s_{i'}} \prod_{i=k+1}^{p-k} \eta_i \frac{1}{s_i}\right),$$

each one with a coefficient $(p!/2^k)^2$. The contribution to the moment is therefore

$$\left(\frac{p!}{2^k}\right)^2 \frac{N^{p-2k}}{(p-2k)!} \frac{S^{2k}(2\phi)}{(k!)^2} = p! \frac{(2k)! C_{2k}^p}{(2^k k!)^2} N^{p-2k} S^{2k}(2\phi).$$

Notice that we have utilized the fact that

$$\sum_{\text{All different } j_i \text{ and } l_i} \left(\prod_{i=1}^k \frac{s_{j_i}^2}{s_{l_i}^2}\right)$$

always contains $S^{2k}(2\phi)/(k!)^2$. Totally, we thus obtain for the leading terms

$$\langle |J(\phi)|^{2p} \rangle = p! N^p \left\{ \sum_{k=0}^{\infty} \frac{(2k)! C_{2k}^p}{(2^k k!)^2} \left[\frac{S(2\phi)}{N} \right]^{2k} \right\}.$$

* Present address.

- ¹ For reviews and further references, see: B.L. Altshuler and P.A. Lee, Phys. Today **41** (12), 36 (1988); G. Bergman, Phys. Rep. **107**, 1 (1984).
- ² For reviews and further references, see: *Hopping transport in solids*, M. Pollak and B.I. Shklovskii, eds. (Elsevier Science, 1991); *Hopping Conduction in Semiconductors*, M. Pollak and B.I. Shklovskii, eds. (North-Holland, Amsterdam, 1990); *Hopping and Related phenomena*, H. Fritzsche and M. Pollak, eds. (World Scientific, 1990); Y. Shapir and X.R. Wang, Mod. Phys. Lett. B **4**, 1301 (1990); B.I. Shklovskii and A.L. Efros *Electronic Properties of Doped Semiconductors* (Springer-Verlag, Berlin, 1984).
- ³ V.L. Nguyen, B.Z. Spivak, and B.I. Shklovskii, Pis'ma Zh. Eksp. Teor. Fiz. **41**, 35 (1985) [JETP Lett. **41**, 42 (1985)]; Zh. Eksp. Teor. Fiz. **89**, 11 (1985) [Sov. Phys. JETP **62**, 1021 (1985)].
- ⁴ E. Medina, M. Kardar, Y. Shapir, and X.R. Wang, Phys. Rev. Lett. **62**, 941 (1989);
- ⁵ U. Sivan, O. Entin-Wohlman, and Y. Imry, Phys. Rev. Lett. **60**, 1566 (1988); O. Entin-Wohlman, Y. Imry, and U. Sivan, Phys. Rev. B **40**, 8342 (1989).
- ⁶ S. Fishman, Y. Shapir, and X.-R. Wang, Phys. Rev. B **46**, 12154 (1992).
- ⁷ E. Medina and M. Kardar, Phys. Rev. Lett. **66**, 3187 (1991); Phys. Rev. B **46**, 9984 (1992).
- ⁸ Y. Meir, N.S. Wingreen, O. Entin-Wohlman, and B.L. Altshuler, Phys. Rev. Lett. **66**, 1517 (1991).
- ⁹ Y. Meir and O. Entin-Wohlman, Phys. Rev. Lett. **70**, 1988 (1993).
- ¹⁰ N.F. Mott, J. Non-cryst. Solids, **1**, 1 (1968).
- ¹¹ V. Ambegaokar, B.I. Halperin, and J.S. Langer, Phys. Rev. B **4**, 2612 (1971).
- ¹² Y.C. Zhang, Europhys. Lett. **9**, 113 (1989); J. Stat. Phys. **57**, 1123 (1989).
- ¹³ E. Medina and M. Kardar, J. Stat. Phys. **71**, 967 (1993).
- ¹⁴ M. Kardar, Nucl. Phys. B **290**, 582 (1987).
- ¹⁵ R. Dashen, J. Math. Phys. **20**, 894 (1979).
- ¹⁶ S. Feng, L. Golubovich, Y.C. Zhang, Phys. Rev. Lett. **62**, 979 (1990).
- ¹⁷ T. Blum, D.S. Koltun, and Y. Shapir, Phys. Rev. Lett. **66**, 2417 (1991); E.H. Lieb and W. Liniger, Phys. Rev. **130**, 1605 (1963).
- ¹⁸ I.S. Gradshteyn and I.M. Ryzhik *Tables of Integrals, Series, and Products* (Academic Press, Orlando, 1980), p.52.

¹⁹ F.P. Milliken and Z. Ovadyahu, Phys. Rev. Lett. **65**, 911 (1990).

²⁰ Y. Zhang, P. Dai, and M.P. Sarachik, Phys. Rev. B **45**, 9473 (1992); Y. Zhang and M.P. Sarachik, *ibid.* **43** 7212 (1991).

²¹ We acknowledge B.L. Altshuler for bringing this point to our attention and E. Medina for clarifying it to us.

²² Y.-L. Lin and F. Nori, Phys. Rev. B **50**, 15953 (1994).

²³ F. Nori and Y.-L. Lin, Phys. Rev. B **49**, 4131 (1994); Y.-L. Lin and F. Nori, Phys. Rev. B **53**,13374 (1996).

²⁴ S.J. Poon, F.S. Pierce, and Q. Guo, Phys. Rev. B **51**, 2777 (1995).

FIGURE CAPTIONS

FIG. 1. (a) Starting from $(0,0)$ on a square lattice, for forward-scattering paths of four steps, electrons can end at five sites: $(4,0)$, $(3,1)$, $(2,2)$, $(1,3)$, and $(0,4)$. Their corresponding $S_{m,n}$ are also shown. The arrows specify the electron hopping directions (only moving to the right and upward are allowed in the directed-path model). Notice that the symmetry $S_{m,n} = S_{n,m}$ holds. $S_{2,2}$ has the strongest interference among them because the number of paths ending at $(2,2)$, and the area they enclose, are both the largest. (b) Six different directed paths connecting $(0,0)$ and $(2,2)$ and their separate phase-factor contributions to $S_{2,2}$; the total equals $1 + 1 + e^{i\phi} + e^{-i\phi} + e^{2i\phi} + e^{-2i\phi} = 2 + 2\cos\phi + 2\cos 2\phi$.

FIG. 2. Plot of m versus $\phi/2\pi$ (denoted by short bars in order to visualize them better), between 0 and 1, such that $I_{2m}(\phi) = 0$; for $m = 1, 2, \dots, 20$. Note that the smallest one is always $1/2m$ and the number of zeros increases rapidly when m becomes larger. The properties of I_{2m} described in Eqs. (19-22) are exhibited in the figure. For instance, when $\phi/2\pi = 1/5$, $I_{2m} = 0$ for $m = 3 + 5n$ and $m = 4 + 5n$ with $n \geq 0$ (namely, $m = 3, 4, 8, 9, 13, 14, 18, 19, \dots$).

FIG. 3. I_{2m} for various m as functions of the flux through each elementary plaquette, $\Phi = \phi/2\pi$ in their respective full period. Notice the 2π (4π) periodicity in ϕ for even (odd) m . In (a), we plot $I_2, I_4, \dots, I_{12}, I_{18}$, and I_{20} . To show the behavior of the rapid small-magnitude fluctuations around zero of $I_{2m}(\Phi)$ for $\frac{1}{2m} \leq \Phi \leq \frac{1}{2}$ when m is even and for $\frac{1}{2m} \leq \Phi \leq \frac{m-1}{2m}$ when m is odd: In (b), we plot I_{10} (top), I_{18} (middle), and I_{38} (bottom) for Φ in their respective interval $[\frac{1}{2m}, \frac{1}{2}]$. In (c), we plot I_{12} (top), I_{20} (middle), and I_{40} (bottom) for Φ in their respective interval $[\frac{1}{2m}, \frac{m-1}{2m}]$. Only some restricted ranges in the vertical axes are exhibited. From these figures, we clearly see the general properties for the behavior of I_{2m} described in Sec. II C.

FIG. 4. $P_{m,m}$ (for $m = 1, 2, \dots, 6$) as functions of the flux through each elementary plaquette, $\Phi = \phi/2\pi$.

FIG. 5. The relative magnetoconductance $\Delta G(\phi)$ versus $\phi/2\pi$ for hopping between $(0,0)$ and $(r/2, r/2)$ for several system sizes. From (a) to (d), the hopping length r corresponds to 4, 10, 20, and 50, respectively. Inserts show $\Delta G(\phi)$ for ϕ between 0 and the corresponding saturated field $\phi/2\pi = 1/2r$. It is observed that for large systems (i.e., r large), $\Delta G(\phi)$ rapidly approaches the saturation value 1 even at $\phi/2\pi$, which is less than $1/2r$.

FIG. 6. (a) ΔG versus $r^{3/2}B$ in 2D with the hopping length $r = 2, 4, \dots, 1000$, and (b) ΔG versus rB in quasi-1D with $r = 2, 3, \dots, 500$, for various small values of B . All the data nicely collapse into a straight line, which verifies the scaling behavior of the small-field ΔG : $(\sqrt{3}/6)r^{3/2}\phi$ in 2D and $(\sqrt{3}/3)r\phi$ for quasi-1D systems. The distance between these data and the solid reference line reflects the prefactor: $\sqrt{3}/6$ in (a) and $\sqrt{3}/3$ in (b).

FIG. 7. Sums over forward-scattering paths between two diagonally-separated sites on a 3D cubic lattice: $\mathcal{I}_3^{\parallel}$ through $\mathcal{I}_{12}^{\parallel}$ for $\mathbf{B} = (\phi, \phi, \phi)$ and \mathcal{I}_3^{\perp} through \mathcal{I}_{12}^{\perp} for $\mathbf{B} = (\phi/2, \phi/2, -\phi)$, as functions of $\phi/2\pi$. Note that while $\mathcal{I}_{3m}^{\parallel}$ has the 2π (4π) periodicity for even (odd) m , \mathcal{I}_{3m}^{\perp} always has a period 4π .

FIG. 8. (a) ΔG versus $r^{3/2}B$ for $\mathbf{B}_{\perp} = B(1/2, 1/2, -1)$, and (b) ΔG versus rB for $\mathbf{B}_{\parallel} = B(1, 1, 1)$ for several values of B and hopping length $r = 3, 6, \dots, 600$. The collapse of all the data into a straight line verifies the scaling of small-field ΔG : $(\sqrt{2}/6)r^{3/2}\phi$ for \mathbf{B}_{\perp} and $(1/3)r\phi$ for \mathbf{B}_{\parallel} . The distance between these data and the solid reference line reflects the prefactor: $\sqrt{2}/6$ in (a) and $1/3$ in (b).

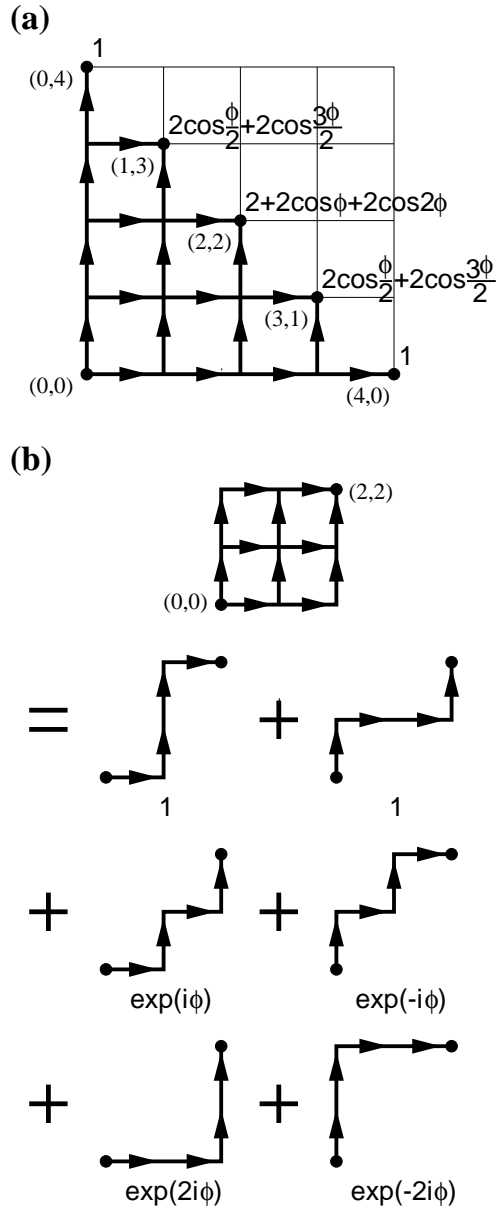


FIG. 1

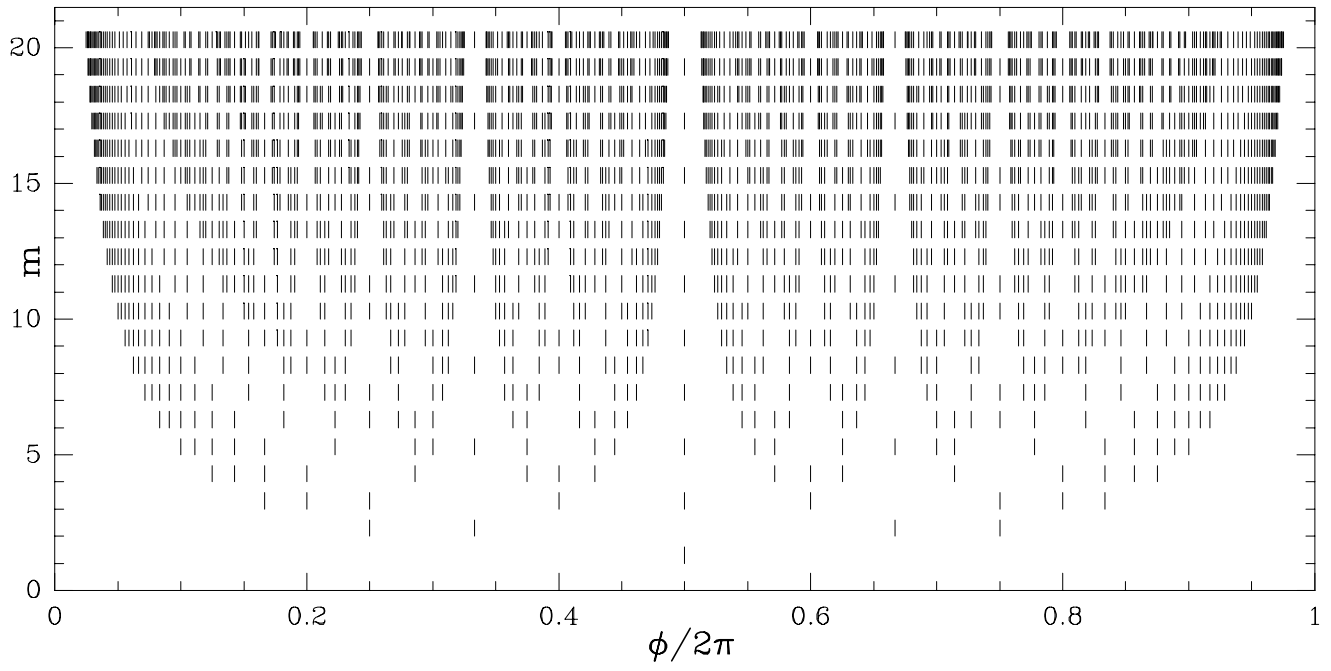


FIG. 2

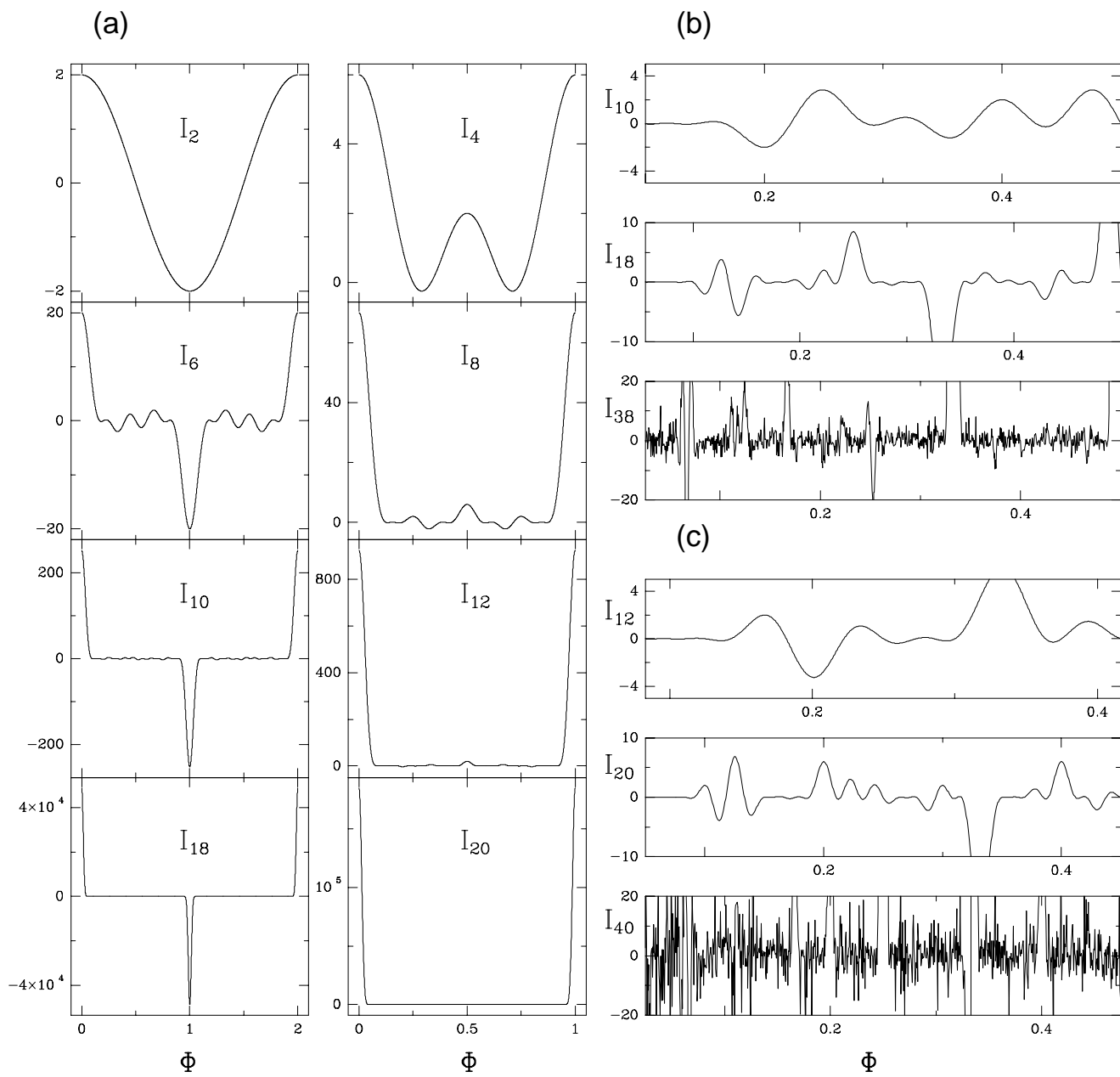


FIG. 3

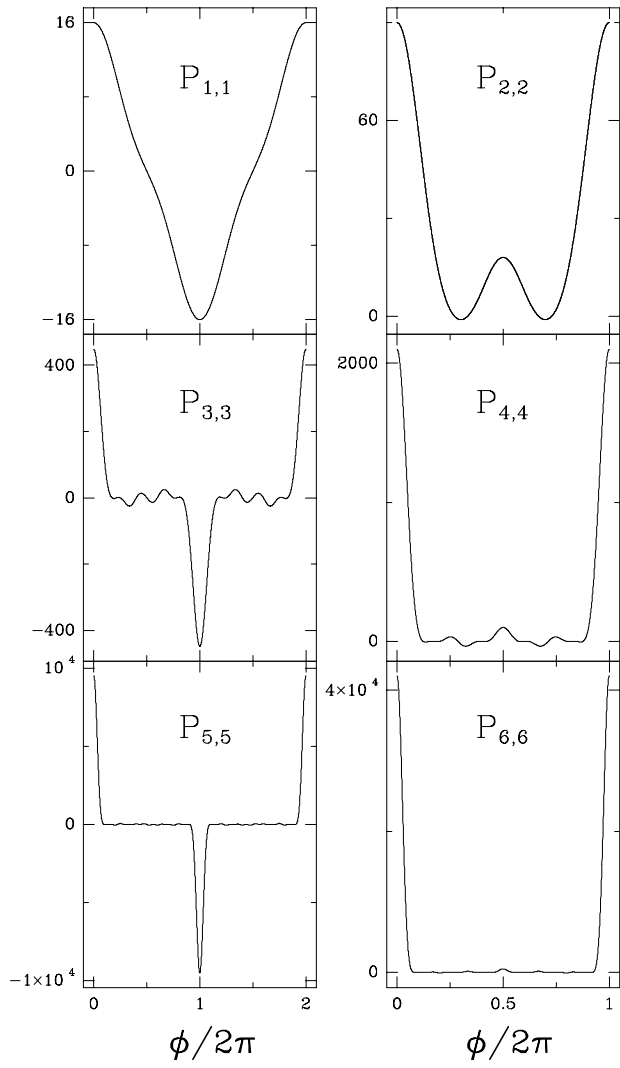


FIG. 4

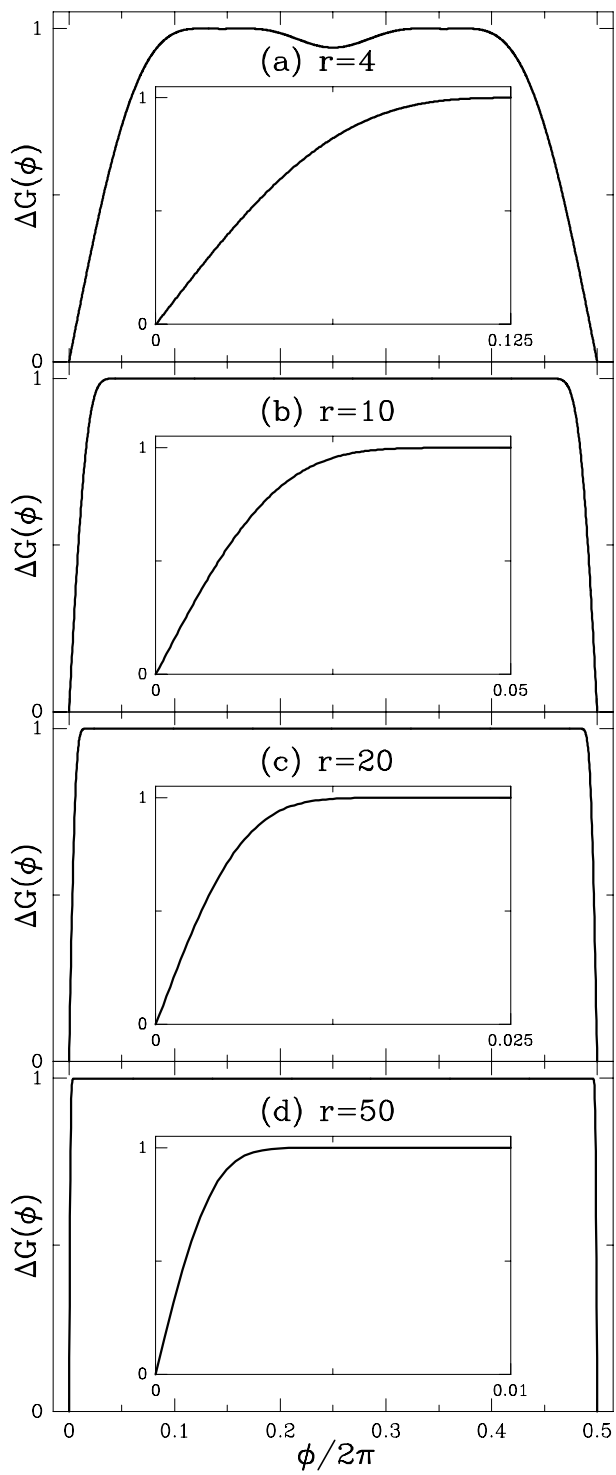


FIG. 5

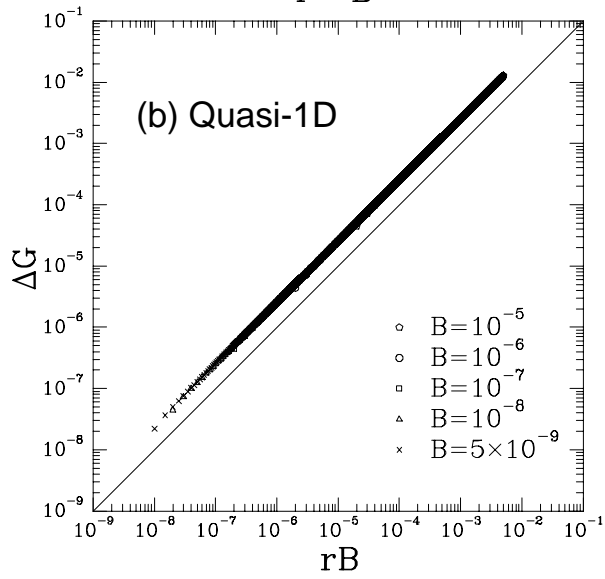
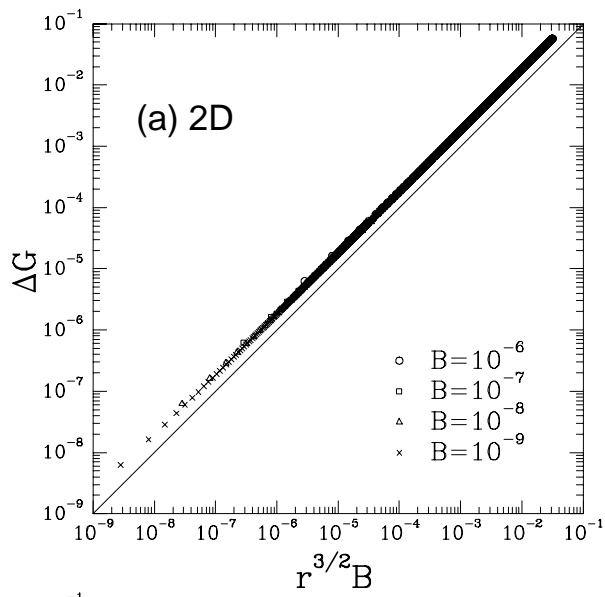


FIG.6

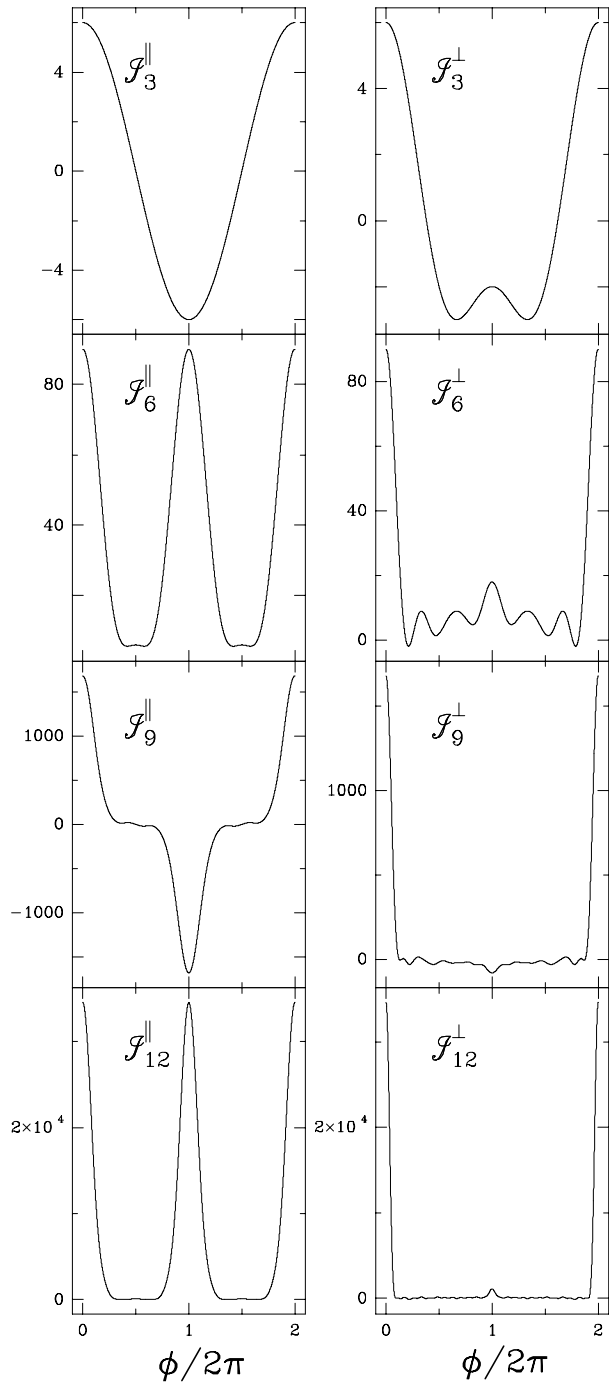


FIG. 7

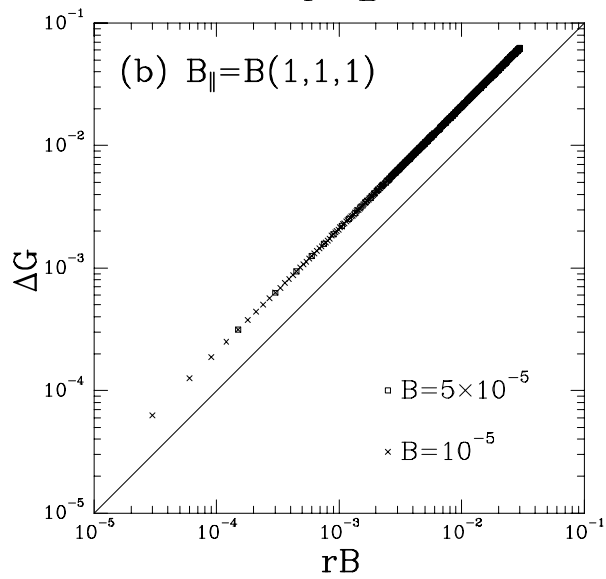
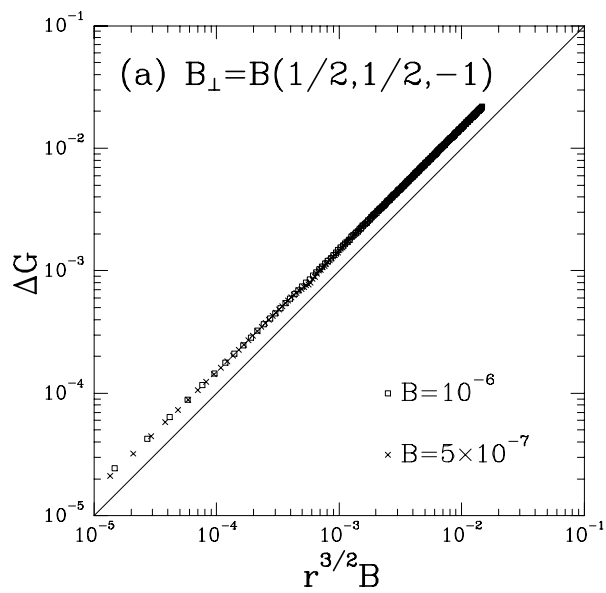


FIG.8